Journal of African Earth Sciences 220 (2024) 105449

Contents lists available at ScienceDirect

Journal of African Earth Sciences

journal homepage: www.elsevier.com/locate/jafrearsci

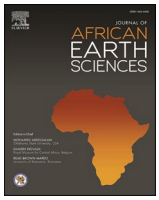

Crustal evolution of alternating Paleoproterozoic belts and basins in the Birimian terrane in southeastern West African Craton

Patrick Asamoah Sakyi [a,b,*], Daniel Kwayisi [a,c], Samuel Nunoo [a,c], Eric Ocran [d], Ben-Xun Su [b], Sanjeewa P.K. Malaviarachchi [e]

[a] Department of Earth Science, College of Basic and Applied Sciences, University of Ghana, Legon-Accra, Ghana
[b] Key Laboratory of Mineral Resources, Institute of Geology and Geophysics, Chinese Academy of Sciences, P.O. Box 9825, Beijing, 100029, China
[c] Department of Geology, University of Johannesburg, Auckland Park Kingsway Campus, South Africa
[d] Department of Statistics and Actuarial Science, College of Basic and Applied Sciences, University of Ghana, Legon-Accra, Ghana
[e] Department of Geology, Faculty of Science, University of Peradeniya, Peradeniya, 20400, Sri Lanka

ARTICLE INFO

Handling Editor: M Mapeo

Keywords:
Birimian granitoids
Continental arc
Crustal reworking
Magmatism
Inherited zircons
Mesoarchean-neoarchean

ABSTRACT

We present a comprehensive review of available geochemical, geochronological and isotopic data on granitoids from the Paleoproterozoic Birimian terrane of Ghana, aimed at providing an in-depth understanding of the geodynamic evolution of southeastern West African Craton. The focus is on plutonic magmatism, crustal recycling and tectonic setting of the granitoids. The granitoids are mainly TTG suites, calc-alkaline granites, diorites, monzonites, two-mica granites and leucogranites. They are characterized by enrichments in LILE and LREE relative to HREE and HFSE. Their variable positive and negative Eu and Sr anomalies and depletions in Nb-Ta and Ti suggest the presence of residual minerals like hornblende and Fe-Ti oxides (e.g., rutile and ilmenite). The plutons probably formed by partial melting of hydrous basaltic/mafic crust metasomatized by slab-derived melts at different depths. The εHf (−14.5 to +7.6) and εNd (−5.3 to +3.5) values and Nd model ages (2.21–2.53 Ga) indicate their crystallization from juvenile magmas derived from a depleted mantle with significant recycling of older crustal material. The older (≥2200 Ma) and younger (<2100 Ma) ages recorded in both belt- and basin-type granitoids indicate that magmatism in both types was contemporaneous. Nonetheless, the basins recorded younger peak emplacement ages compared to adjacent belts. The presence of inherited older zircon grains (Archean zircon cores?), is widespread in southeastern WAC. The granitoids formed in a continental arc setting via subduction–accretion processes. Furthermore, the magmatic time-span is more prolonged in southern Ghana, with the sedimentary basins recording the longest intervals of magma emplacement. The sub-chondritic εHf data and Hf model ages strongly suggest the existence of Neoarchean to Mesoarchean crustal material in eastern Ghana during the Birimian crust formation. We propose that the subduction-accretion processes during the Paleoproterozoic Eburnean orogeny in the WAC contributed to the formation of the Columbia supercontinent in the Late Paleoproterozoic-Mesoproterozoic.

1. Introduction

Granitoids are the most common and essential constituents of the continental crust as these are often associated with or host important economic mineralization (Taylor and McLennan, 2009; Sial et al., 2011; Rudnick and Gao, 2014; Janoušek and Moyen, 2019). They represent the final products of crust-mantle differentiation through partial melting and fractional crystallization along mature arcs and convergent plate margins (e.g., Grove et al., 2003; Chappell, 2004; Jagoutz and Klein, 2018; Sawyer et al., 2011; Wu et al., 2017; Zheng and Gao, 2021). The sources of granitoids exhibit considerable variability, ranging from predominantly crustal- to mantle-derived materials (Pearce, 1996). The compositions of granitoids in continental provinces are primarily determined based on the nature of the source material, residual and peritectic minerals of the melts, and the passage of travel of the melt (Zheng and Gao, 2021). Granitoid plutons, which are highly compositionally diverse, form essential constituents of the continental crust and orogenic zones (Altherr et al., 2000; Eleftheriadis and Koroneos, 2003).

* Corresponding author. Department of Earth Science, College of Basic and Applied Sciences, University of Ghana, Legon-Accra, Ghana.
E-mail address: pasakyi@ug.edu.gh (P.A. Sakyi).

https://doi.org/10.1016/j.jafrearsci.2024.105449
Received 25 April 2024; Received in revised form 21 August 2024; Accepted 11 October 2024
Available online 15 October 2024
1464-343X/

Many studies have been carried out in an attempt to elucidate the origin of granitoids (e.g., Soesoo, 2000; Chappell and White, 2001; Brown, 2013; Moyen et al., 2017; Bonin et al., 2020; Tang et al., 2021; Zheng and Gao, 2021; Zhong et al., 2023). Nevertheless, their classifications and petrogenetic mechanisms remain topics of continuous debate. So far, the two proposed mechanisms are; partial melting of crustal lithologies (e.g., Chappell and White, 1974; White and Chappell, 1983; Chappell, 1984; Chappell et al., 1988; Arndt, 2013; Aidoo et al., 2020; Aidoo et al., 2021; Tang et al., 2021), and fractional crystallization via melting of the mantle (e.g., Clemens and Wall, 1984; Chappell et al., 1987; Collins, 1996; Soesoo, 2000; Rapp et al., 2000; Macpherson et al., 2006). The controversies surrounding the origin and petrogenesis of granitoids stem from the fact that some granitoids within accretionary-collisional zones exhibit juvenile isotopic signatures, resembling typical characteristics of mantle-derived rocks. This phenomenon has given rise to the hypothesis that collisional zones are important sites for the net growth of the continental crust (Mo et al., 2008; Niu et al., 2013; Chen et al., 2015; Moyen et al., 2017; Moyen, 2020; Xiao et al., 2020). The Paleoproterozoic Birimian granitoids are, therefore, no exemption from these controversies.

The study of Precambrian terranes is very crucial to aid our understanding of the tectonic evolution of the Earth since these terranes mark the transition from an early-Earth to a state of modern-day cratonic preservation with stiff roots composed of feasible buoyant mantle material (Kearey et al., 2009; Roverato et al., 2019). The Paleoproterozoic Birimian terrane of the West African Craton (WAC) (Fig. 1) represents a good example of Precambrian terranes that bridges a significant gap in crustal evolution and mantle activity for a period considered to be associated with global magmatic quiescence on other well-studied continents (Abouchami et al., 1990; Condie et al., 2009). The Birimian of the WAC also represents a suitable target to explore the unresolved issues regarding rates of early crustal growth and accretion during the transitional Archean-Proterozoic period (Abouchami et al., 1990; Drummond and Defant, 1990).

The combination of geochemical data, zircon U-Pb dating and radiogenic isotopes systematics of granitoids can provide reliable information about their petrogenesis, magma source characteristics, the tectonic regime where granitoids were developed, and their role in crustal growth in both space and time (e.g., Anum et al., 2015; Kemp et al., 2007; Gong et al., 2019; Spencer et al., 2019). For example, the combined application of U-Pb ages and Lu-Hf isotope systematics in igneous zircon allows to investigate crust production, recycling and preservation events, mapping juvenile vs recycled crustal fragments, and characterizing magma sources (Champion and Sheraton, 1997; Amelin et al., 1999, 2000; Rino et al., 2004; Condie et al., 2005; Hawkesworth and Kemp, 2006; Czarnota et al., 2010; Laurent and Zeh, 2015). Thus, combined U-Pb and Lu-Hf isotopic studies help to investigate the applicability of plate tectonic models through the Earth history, especially if they are coupled to petrogenetic information about the zircon-hosting rocks (Laurent and Zeh, 2015). Geochemical data, including major and trace element compositions and radiogenic isotopes, help distinguish among different petrogenetic processes, source materials (crustal material, mantle-derived magma, or a combination of both) and tectonic settings in which granitoids form (e.g., Whalen et al., 1987; Pearce, 1996; Moyen, 2009; Collins et al., 2019). Similarly, oxygen isotope systematics of granitoids has also provided a window to unravel geotectonic processes, provided evidence of juvenile crust recycling, and aided in understanding the evolution of the continental crust (e.g., Bruand et al., 2019). Thus, granitoids contain useful information that often addresses highly debatable issues on global plate tectonic regimes in the early Paleoproterozoic period (Gong et al., 2019).

The Paleoproterozoic Birimian terrane of the WAC has received considerable attention in research studies due to its critical implications for both precious and base metals (e.g., Lompo, 2009; Nyame, 2013; Sakyi et al., 2014; Grenholm et al., 2019). The Birimian terrane contains various generations of granitoids that formed during the Eburnean orogeny at ca. 2.2-2.05 Ga (e.g., Hirdes et al., 1992; Baratoux et al.,

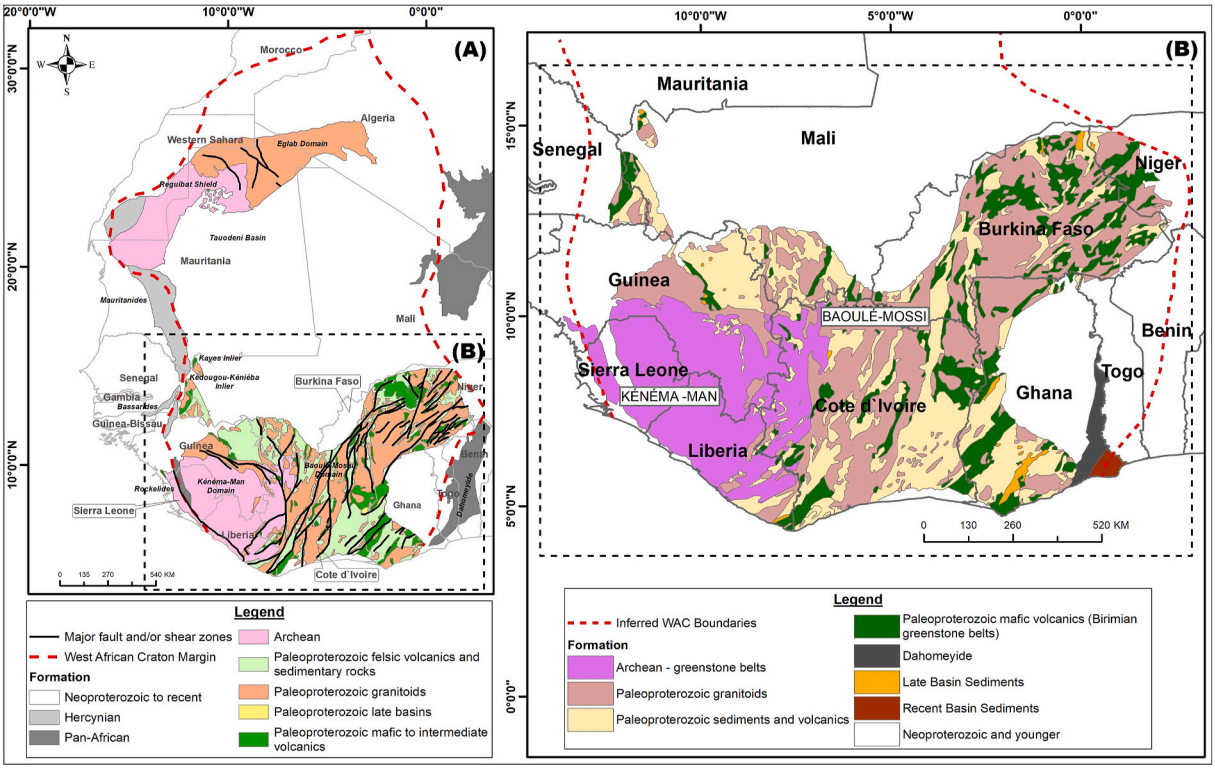

Fig. 1. Simplified geological map of (a) the entire West African Craton and (b) the southern part of the craton showing the Kénéma-Man Archean and the Paleoproterozoic Baoulé-Mossi domains (after Robertson and Peters, 2016).

2011; de Kock et al., 2011; Sakyi et al., 2014; Anum et al., 2015; Grenholm et al., 2019; Amponsah et al., 2023). Recent studies have highlighted the juvenile nature of the Birimian terrane in Ghana and also identified significant levels of ancient lithospheric recycled materials (e.g., Doumbia et al., 1998; Hirdes and Davis, 2002; Gasquet et al., 2003; Dampare et al., 2008; Baratoux et al., 2011; Sakyi et al., 2014; Amponsah et al., 2023). However, the geodynamic evolution, tectonic regime and origin of granitoids during the Eburnean Orogeny are debated (Feng et al., 2018). Although it is widely accepted that the Birimian granitoids formed through subduction-accretion process (e.g., Sakyi et al., 2014; Anum et al., 2015; McFarlane et al., 2019a,b), the nature of this subduction zone (continental-arc versus oceanic-arc) remains enigmatic. This contribution presents a review of existing literature on Birimian granitoids of southeastern WAC with emphasis on Ghana, highlighting their origin and possible interaction between juvenile magma sources and crustal components and the possibility of Archean crustal reworking during the magmatic events that resulted in the formation of the granitoids. The review is aimed at putting further constraints on our understanding of the tectonic setting and evolution of the Birimian terrane and the WAC.

2. Geological setting

2.1. Paleoproterozoic Birimian rocks of the West African craton

The Precambrian West African Craton (WAC) consists of two Archean nuclei juxtaposed against multiple Paleoproterozoic domains made up of greenstone belts, sedimentary basins, regional tonalite-trondhjemite-granodiorite (TTG) granitoid plutons and large-scale shear zones, overlain by Neoproterozoic and younger sedimentary basins (e.g., Egal et al., 2002; Pouclet et al., 2006; Baratoux et al., 2011; Jessell and Liégeois, 2015). These Archean-Paleoproterozoic domains form the Reguibat shield in the north and Leo-Man shield in the south of the WAC, separated by the Neoproterozoic-Palaeozoic Taoudeni basin and outlined by the Neoproterozoic and Cenozoic Pan-African and Hercynian mobile belts (Fig. 1a) (Abouchami et al., 1990; Villeneuve and Cornee, 1994; Egal et al., 2002; Deynoux et al., 2006; Pouclet et al., 2006; Ennih and Liégeois, 2008; Petersson et al., 2018). Within the Taoudeni basin occurs the Paleoproterozoic Kedougou-Kéniéba Inlier (KKI) in Senegal and Kayes Inlier (KI) in Mali, suggesting that the Taoudeni basin overlies the Birimian terrane (e.g., Boher et al., 1992; Ennih and Liégeois, 2008; Baratoux et al., 2011). The southern Leo-Man shield of the WAC is divided into a western Archean crustal block called the Kénéma-Man shield characterized by Liberian (ca. ~2.75 Ga), Leonian (ca. ~2.95 Ga) and pre-Leonian (ca. ~3.1 Ga) orogenic events (Wright et al., 1985), and a central-eastern domain (Baoulé-Mossi/Birimian of Paleoproterozoic age) characterized by the Eburnean (ca. ~2.2-2.0 Ga) orogeny (e.g. Feybesse et al., 2006; Vidal et al., 2009; Hein, 2010; de Kock et al., 2011). The Archean and Paleoproterozoic domains have been affected by three main tectono-magmatic and metamorphic events, namely; the Leonian event at ~3200–3000 Ma, the Liberian event at ~2900–2700 Ma, and the Eburnean orogeny at ~2250–2060 Ma (e.g., Baratoux et al., 2011; Tshibubudze et al., 2013; Sakyi et al., 2014; Anum et al., 2015; Kouamelan et al., 2015; Block et al., 2016a).

The Paleoproterozoic Birimian rocks of the West African Craton (WAC) crop out extensively in Ghana, Cote d'Ivoire, Mali, Niger, Burkina Faso and, to a limited extent, Senegal, Guinea, and Mauritania (Fig. 1b). These rocks occupy nearly two-thirds of the WAC and record an extensive episode of continental crust formation in the early part of the Proterozoic (Attoh and Ekwueme, 1997). The Birimian terrane in the southeastern portion of the WAC is referred to as the Baoulé-Mossi domain (Fig. 1b) and comprises ~2.25–1.98 Ga greenstone (volcanic) belts separated by sedimentary basins. All were intruded by granitoids, which were subjected to greenschist to amphibolite facies and granulite facies metamorphism, especially at pluton contacts (e.g., Milési et al., 1989; Boher et al., 1992; Ama-Salah et al., 1996; Hirdes et al., 1996; Peucat et al., 2005; Feybesse et al., 2006; de Kock et al., 2009; Baratoux et al., 2011).

The Paleoproterozoic Birimian rocks in Ghana are exposed in a third of the country (Fig. 2). The terrane is characterized by successions of sub-parallel, linear greenstone belts, namely; Kibi-Winneba, Ashanti, Sefwi, Bui, Bole-Nangodi (all of which trend NE-SW) and the N-S trending Lawra Belt, separated by metasedimentary basins (Suhum, Cape Coast, Kumasi, Sunyani, and Maluwe basin) at roughly regular intervals (e.g., Leube et al., 1990; Sylvester and Attoh, 1992; Hirdes et al., 1996; Sakyi et al., 2014, 2020a; Block et al., 2016b; Senyah et al., 2016; Kazapoe et al., 2022, 2023), and intruded by several suites of syn-to late-stage Eburnean granitoids (Fig. 2) (e.g., Leube et al., 1990; Hirdes et al., 1992; Feybesse et al., 2006; Thiéblemont et al., 2004; Sakyi et al., 2014; Amponsah et al., 2023).

Between 2.14 and 2.10 Ga, during the Eburnean orogeny, the early Palaeoproterozoic crust that had formed between 2.20 and 2.14 Ga underwent reworking (Sakyi et al., 2014; Anum et al., 2015; Block et al., 2016b; Block et al., 2015; Block et al., 2016a; Amponsah et al., 2023). Granitoid intrusions and the development of greenstone belts were two features of the Older Eburnean phase (EoEburnean, 2.3–2.14 Ga). The

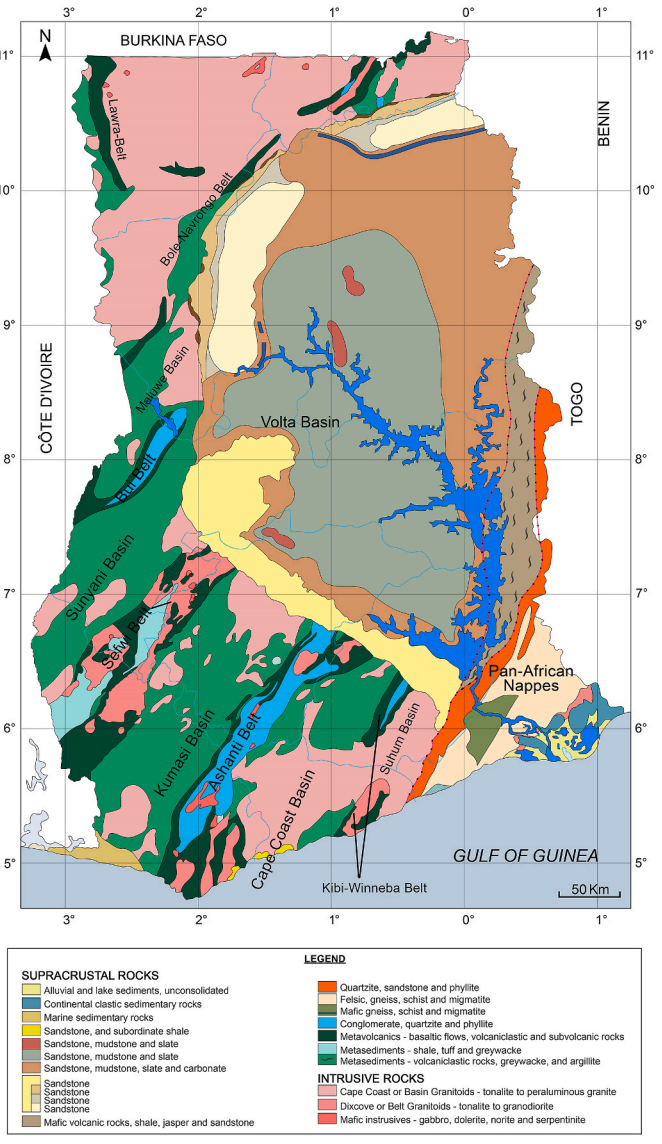

Fig. 2. Simplified geological map of Ghana showing the Paleoproterozoic Birimian belts and basins (after Petersson et al., 2016).

West African Craton stabilized as a result of the major volcanic and plutonic activity that was linked to this period. During this time, the formation of shear zones at the regional scale, metamorphism, and crustal thickening dominated the tectonic processes (Oberthür et al., 1998; Loh et al., 1999; Perrouty et al., 2012; Sakyi et al., 2014). The Younger Eburnean phase (2.14–2.0 Ga) involved further deformation, metamorphism, and magmatism. This phase was marked by more intense folding, faulting, and the emplacement of late-stage granitic intrusions. The Younger Eburnean represents the final stages of cratonization in West Africa, leading to the stabilization of the crust and the formation of major mineral deposits, including gold (Amponsah et al., 2015; Amponsah et al., 2023).

The greenstone belts comprise tholeiitic basalts and pillow lavas superimposed by calc-alkaline andesites, dacites, rhyolites and tuffs interbedded with volcaniclastics sedimentary rocks (Abouchami et al., 1990; Leube et al., 1990; Boher et al., 1992; Milési et al., 1992; Sylvester and Attoh, 1992; Agra et al., 2023). Subsequent, local small ultramafic bodies intruded the volcanic rocks (e.g., Dampare et al., 2008). The metasedimentary basins contain greywackes, shales and siltstones, phyllites, cherts, argillites, volcaniclastics and chemical sedimentary rocks (Leube et al., 1990; Sakyi et al., 2018, 2019, 2020a), which, during isoclinal folding, obtained a phyllitic texture. Some studies have proposed that volcanic rocks of the Birimian greenstone belts and the metasedimentary rocks were formed contemporaneously as lateral facies equivalents during the Eburnean event (e.g., Leube et al., 1990; Feybesse et al., 2006). Other studies postulated that eruption of the Birimian volcanic belts, emplacement of the older granitoid rocks, and an earlier episode of metamorphism, uplift, and erosion occurred during Eburnean 1 orogeny between ca. 2240 and 2150 Ma, whereas the deposition of the Birimian sedimentary rocks and Tarkwaian Group occurred between ca. 2130–2116 Ma (e.g., Allibone et al., 2002a,b).

Unconformably overlying the Birimian terrane are the Tarkwaian sedimentary sequences, which contain clasts of rocks representative of the Birimian sequences. The Tarkwaian is considered a molasse deposit of non-marine origin, derived from rapid erosion of Birimian crust. The unit was deposited proximally in an elongate, intra-montane basin. Zircon studies by various researchers (e.g., Leube et al., 1990; Eisenlohr and Hirdes, 1992; Davis et al., 1994; Pigois et al., 2003; Feybesse et al., 2006) obtained ages ranging between 2.14 Ga and 2.10 Ga, representing the crystallization of magmatic rocks in the source region. Evolution of the Maluwe basin and overlying molasses of the Banda Group in the Bui belt (de Kock et al., 2012) was due to the northward convergence and thrusting of the Maluwe basin onto, and forming an orogenic continental arc along the southern edge of the Bole-Navrongo terrane. Associated deformation and magmatism (Tanina Suite: 2126-2120 Ma) illustrate the creation of a short-lived orogenic event. Petersson et al. (2016) re-evaluated the results of the above researchers and concluded that the Tarkwa Group contains detrital zircons of Eoeburnean ages (>2145 Ma), a huge detrital zircon population with ages of the Tanina Suite (2126-2120 Ma) and even younger ages (<2097 Ma) which determine the deposition thereof to be after 2097 Ma. This implies that the molasse sequences are not all related to a singular orogenic event. Thus, the creation of the Tanina magmatic arc marks the onset of the Eburnean tectonogenesis that led to the contraction of the post-Eoeburnean sedimentary depositories.

2.2. Birimian granitoids of Ghana

The tonalite-trondjhemite-granodiorite (TTG) granitoid plutons associated with the Birimian terrane of Ghana historically, irrespective of age, were grouped into four, namely: Cape Coast, Winneba, Bongo, and Dixcove type granitoids (Pohl, 1998 and references therein). The Cape Coast-type granitoids are a foliated, biotite (±muscovite)-bearing rocks, chiefly consisting of biotite-granodiorites and granites. This groups is interpreted as pre- or syntectonic with peraluminous characteristics and largely intrudes the sedimentary basins (e.g. Leube et al., 1990; Eisenlohr and Hirdes, 1992; Hirdes et al., 1992; Taylor et al., 1992). The Dixcove-type, again, usually intrudes the greenstone belts, and are comprised predominantly of massive hornblende-bearing tonalites and post-tectonic granodiorites with metaluminous affinities (Leube et al., 1990; Hirdes et al., 1992; Taylor et al., 1992). The Winneba and the Bongo/Banso granitoids occur as isolated intrusions (e.g. Leube et al., 1990; Petersson et al., 2016). The Bongo-type granitoid, referred to as Lambo River alkali granite (de Kock et al., 2011, 2012), is a post-orogenic intrusion that cuts across the Tarkwaian strata located in northern Ghana. These granitoids are marked by distinct pinkish coloration due to the presence of potassium-rich feldspars (e.g., Leube et al., 1990; Abitty et al., 2016; Sakyi et al., 2020a). The Winneba-type are granodioritic to granitic in composition. Its distribution is limited to a small area close to Winneba in southeastern Ghana, where its whole-rock Sm-Nd and zircon Hf isotopic model ages of 2.6 Ga suggest Archean crust involvement (Taylor et al., 1992; Petersson et al., 2016). Syn-to post-orogenic magmatism invaded the volcano-sedimentary rocks of Ghana during the entire period of the Eburnean orogeny (Allibone et al., 2002a; Baratoux et al., 2011). Since it was a multistage event, de Kock et al. (2011, 2012) grouped the igneous rocks, irrespective of their composition, according to their age and place in the geological evolution. In these studies, however the igneous rocks were grouped according to region, irrespective of age or composition.

3. Results

3.1. Whole-rock geochemistry

Geochemical studies conducted on the Paleoproterozic Birimian plutonic suites in Ghana so far have produced similar results. The whole rock major and trace elements data for the Birimian granitoids of Ghana are presented in Supplementary Table S1. The data covers a total of 211 samples from all the basins and belts, except the Bui belt. Granitoids from the greenstone belts have intermediate to high SiO_2 contents in the range of 55.20–81.89 wt% (average = 68.63 wt%), low to high alkali contents with K_2O values of 0.83–5.58 wt% (average = 3.07 wt%) and Na_2O values of 2.93–5.97 wt% (average = 4.29 wt%). Their total alkalis ($K_2O + Na_2O$) vary from 4.44 to 9.55 wt% (average = 7.36 wt%) with Na_2O/K_2O ratios of 0.65–5.80. They are characterized by low to intermediate contents of Fe_2O_3 (0.27–8.04 wt%; average = 3.34 wt%), CaO (0.44–7.20 wt%; average = 2.77 wt%), and MgO (0.03–6.50 wt%; average = 1.39 wt%), and low P_2O_5 (0.01–0.74 wt%), TiO_2 (0.02–1.08 wt%), and MnO (0.01–0.14 wt%). Al_2O_3 content varies from 10.94 to 17.30 wt% (average = 14.62 wt%) (e.g., Dampare et al., 2005; Grenholm, 2011; Sakyi et al., 2014; Anum et al., 2015; Abitty et al., 2016; Block et al., 2016b; McFarlane et al., 2019b; Sakyi et al., 2020a).

Similarly, granitoids from the sedimentary basins have SiO_2 contents varying from 51.50 to 81.79 wt% (average = 67.73 wt%). They also display low to high K_2O contents of 0.51–5.97 wt% (average = 2.29 wt%) and Na_2O contents of 1.99–5.66 wt% (average = 4.30 wt%). The rest of the major oxides are low to high contents of MgO (0.08–13.65 wt%; average = 1.77 wt%), and Fe_2O_3 (0.57–16.03 wt%; average = 3.79 wt%), and low concentrations of P_2O_5 (0.01–0.89 wt%), TiO_2 (0.04–2.83 wt%), and MnO (0.00–0.24 wt%). Their Al_2O_3 contents are in the range of 9.38–18.40 wt% (average = 15.13 wt%). Their total alkalis ($K_2O + Na_2O$) vary from 3.89 to 9.06 wt% (average = 6.60 wt%) with Na_2O/K_2O ratios of 0.45–7.06 (e.g., Dampare et al., 2005; Grenholm, 2011; Sakyi et al., 2014; Anum et al., 2015; Abitty et al., 2016; Block et al., 2016b; McFarlane et al., 2019b; Sakyi et al., 2020a). Based on the major element Harker diagrams (Figs. 3 and 4), the granitoids generally display negative linear trends. Notably the plots of SiO_2 vs. Fe_2O_3, MgO, CaO, Al_2O_3, P_2O_5, and TiO_2, show negative linear correlations (Figs. 3 and 4). In contrast, the SiO_2 vs. Na_2O and SiO_2 vs. K_2O plots exhibit diffuse patterns in the belt-type granitoids (Fig. 3) and slightly positive correlations are displayed in the SiO_2 vs. Na_2O and SiO_2 vs. K_2O plots for the basin-type granitoids (Fig. 4). The granitoids are mostly

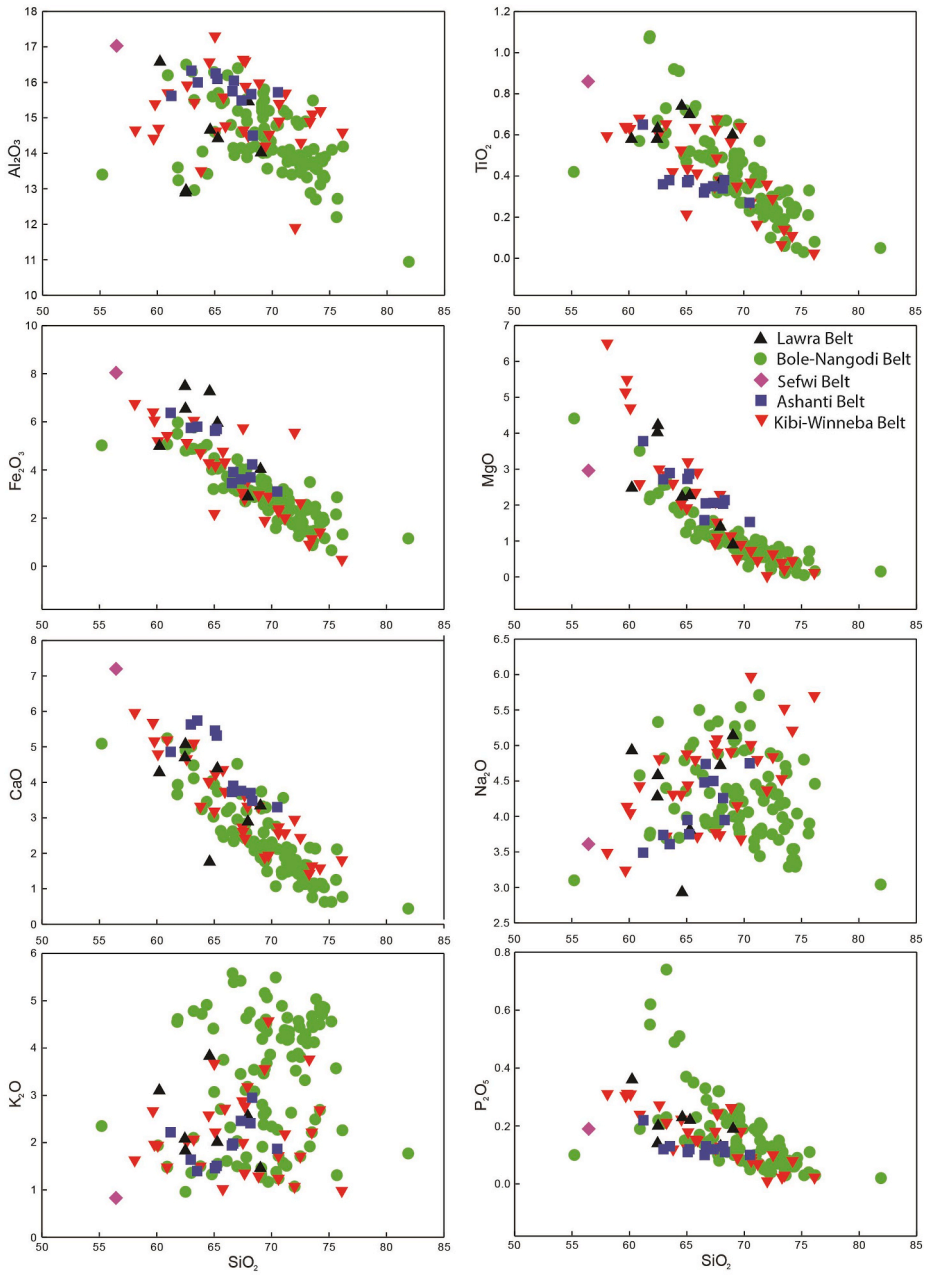

Fig. 3. Variation in major elements with SiO_2 for the belt-type Birimian granitoids of Ghana. Data sources are: Dampare et al. (2005); Grenholm (2011); Sakyi et al. (2014); Anum et al. (2015); Abitty et al. (2016); Block et al. (2016b); Sakyi et al. (2020a).

metaluminous to slightly peraluminous (Fig. 5a), and plot mainly in the fields of granite, granodiorite, tonalite, monzonite, trondhjemite, and diorite. The granitoids of the Ashanti belt are more restricted to the fields of tonalite and granodiorite (Figs. 5b and 6b). They plot mainly in the calc-alkaline series (Fig. 6a), except those from the Suhum basin and Bole-Nangodi belt that also have shoshonitic affinity (Fig. 5c).

The granitoids are enriched in LILE and LREE relative to HREE and HFSE, and display negative Nb-Ta anomalies, pronounced negative Ti and P anomalies, enriched Zr–Hf, and variable positive and negative Eu and Sr anomalies (Figs. 7–10). There are generally positive anomalies of Rb, Ba, U, and Pb in all the samples, except the data for Ashanti belt, Sefwi belt, Sunyani basin and Cape Coast basin in which Pb was not analysed. The Eu anomalies (Eu/Eu*) range from 0.13 to 1.70 for the belt-type granitoids and 0.28–2.25 for the basin-type granitoids (Figs. 7 and 8). On the chondrite-normalized REE diagrams (Figs. 9 and 10), they show strongly fractionated REE patterns, with LREE-enrichment $(La/Yb)_N$ of 0.94–252.97 and 3.49–111.98 for belt-type and basin-type granitoids, respectively, whilst recording HREE-fractionation $(Gd/Yb)_N$ of 0.69–14.11 and 1.14–11.25 98 for belt-type and basin-type granitoids, respectively.

3.2. U-Pb data, Lu-Hf and Sm-Nd isotope systematics

In recent years, coupled U-Pb ages and Lu-Hf isotope systematics was used to better understand the source and petrogenesis of magmas that formed the Paleoproterozoic Birimian rocks of southeastern WAC. A summary of U-Pb and related ages for Birimian granitoids in Ghana are presented in Table 1, and details are listed in Supplementary Table S2. The ages are displayed on the geological map of the Birimian in Ghana (Fig. 11). Also presented is a summary of εHf data in Table 3, with details in Supplementary Table S3. εHf data range from −14.5 to +7.6. Additionally, other Birimian granitoids ages are listed in Table 2. Ages of

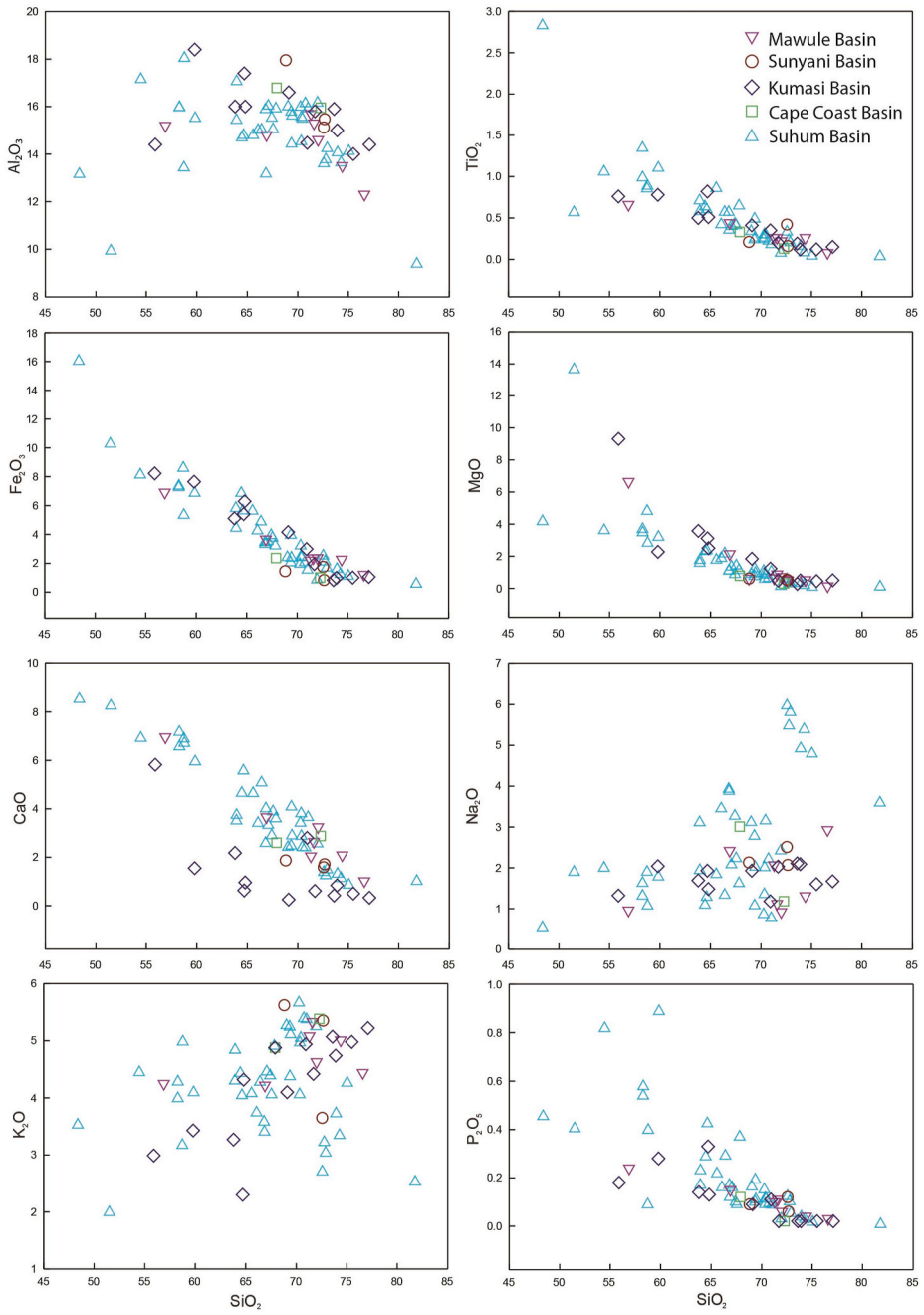

Fig. 4. Variation in major elements with SiO_2 for the basin-type Birimian granitoids of Ghana. Data sources are: Grenholm (2011); Losiak et al. (2013); Block et al. (2016b); (Kwayisi et al.,)(unpublished).

plutonic suites of the Proterozoic Birimian terranes of Ghana span the range of ca. 2232-2058 Ma (for zircon grains) and ca. 2222-1907 Ma for other minerals (monazite, titanite, rutile, galena, muscovite, biotite and amphibole) (Table 1). A plot of εHf vs. ages of Birimian granitoids is shown in Fig. 12. These age brackets and εHf data significantly overlap each other. Exceptions are the K-Ar ages of biotite/muscovite obtained by Chalokwu et al. (1997) that extend to much younger value of ca. 1907 Ma.

3.3. Age relationship between belts and basins

The age data is presented in histograms (Fig. 13), showing the frequency of occurrence of the ages. The histograms reveal that the ages are dominated by those in the age bracket of ca. 2100–2200 Ma. The peak ages are; 2063 Ma (Cape Coast basin), 2087 Ma (Sunyani basin), and 2129–2161 Ma for the rest of the domains. The data does not clearly distinguish between the relative ages of belt- and basin-type granitoids. For example, older crystallization ages ≥2200 Ma have been reported in both the greenstone belts and sedimentary basins as follows; ca. 2228 - 2211 Ma (Lawra and Bole-Nangodi belts; Sakyi et al., 2014; Block et al., 2016b; Nunoo et al., 2022), ca. 2219 - 2200 Ma (Kibi-Winneba belt; Feybesse et al., 2006; Petersson et al., 2018), ca. 2222 Ma (Sefwi belt; Feybesse et al., 2006), and ca. 2232 - 2224 Ma (Suhum basin; Grenholm, 2011, Petersson et al., 2016; Amponsah et al., 2023) (Table 1, Supplementary Table S2). Likewise, younger crystallization ages <2100 Ma have also been reported in both belt- and basin-type granitoids. These include; ca. 2092–2058 Ma (Ashanti belt; Oberthür et al., 1998; Parra-Avila et al., 2018), ca. 2090 Ma (Kibi-Winneba belt; Grenholm, 2011), ca. 2019–1907 Ma (Cape Coast basin, Chalokwu et al., 1997), ca. 2092–2073 Ma (Sunyani basin; Hirdes et al., 1992; Petersson et al.,

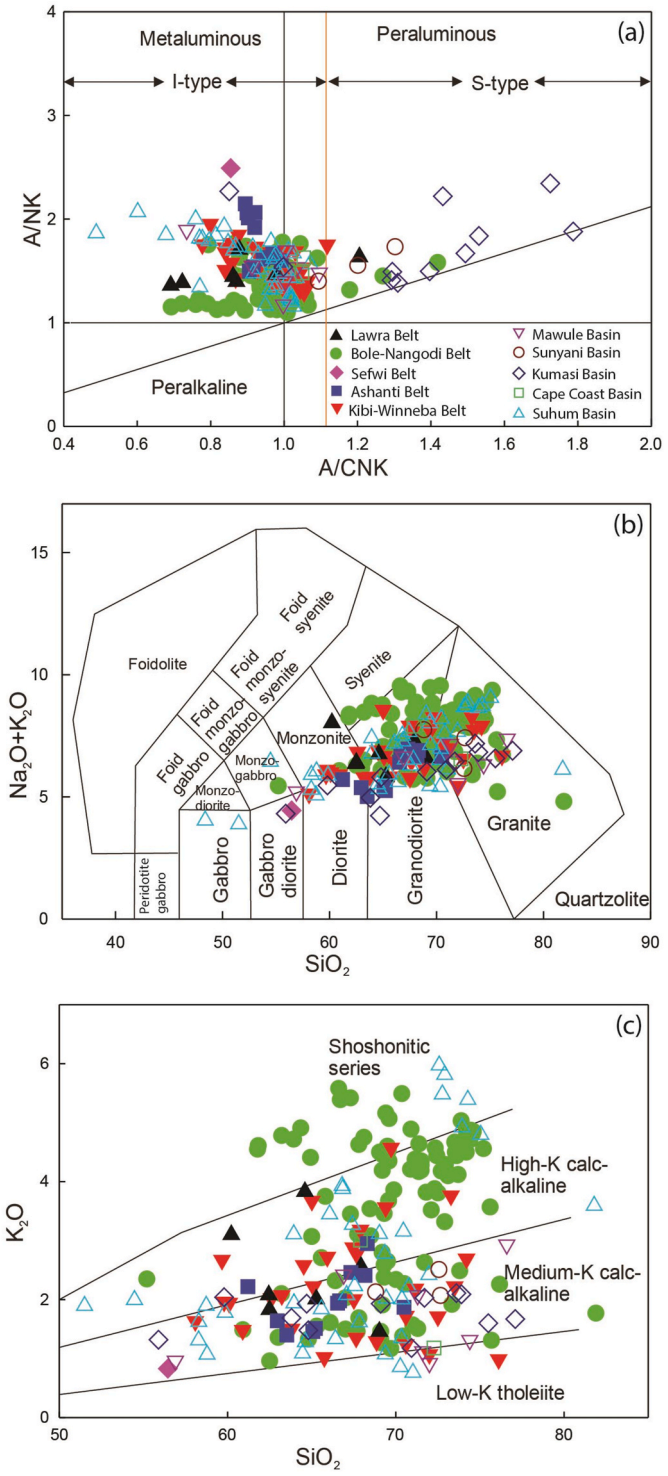

Fig. 5. (a) Alumina saturation vs. alkalinity diagram (after Maniar and Piccoli, 1989); (b) TAS diagram (Middlemost, 1994); and (c) K_2O vs. SiO_2 diagram (Peccerillo and Taylor, 1976) for the Birimian granitoids of Ghana. Data sources as in Figs. 3 and 4.

2016, McFarlane, 2018), ca. 2085 Ma (Suhum basin; Amponsah et al., 2023), and ca. 2092 Ma (Kumasi basin; Losiak et al., 2013) (Table 1, Supplementary Table S2). This finding is at variance with the two schools of thought regarding the relative ages of the basin- and belt-type granitoids as follows: (i) the belt-type granitoids are older than the basin-type granitoids and the belt-type granitoids are approximately coeval and comagmatic with volcanic rocks of the Birimian Supergroup, while the basin plutons were intruded toward the end of Eburnean and postdate the Tarkwaian sedimentation (e.g., Hirdes et al., 1992), (ii) the basin-type granitoids are syn-orogenic foliated batholiths occurring in the central portions of Birimian sedimentary basins, whereas the belt-type granitoids are mostly late-orogenic unfoliated intrusions in greenstone belts (Leube et al., 1990). Some authors have invoked gravity-driven vertical movements of dense greenstone belts and buoyant granitoid domains, based on monotonous metamorphism, increasing only in granitoid contact aureoles, and interpreted as dome and basin geometry (Pons et al., 1995; Vidal et al., 2009). This model describes the exhumation of migmatitic rocks, interpreted as the product of buoyancy-driven ascent in a rheologically weak, hot orogenic crust, following homogeneous and distributed crustal thickening and extensive granitoid emplacement (e.g. Caby et al., 2000; Ganne et al., 2014; Pouclet et al., 1996; Vidal et al., 2009; Ganne et al., 2014).

The available age data strongly suggest that the evolution of both belt- and basin-type granitoids were contemporaneous. That notwithstanding, the peak ages indicate that, largely the basins recorded lower magmatic peak ages than the adjacent belts (Fig. 13).

The Birimian granitoids of Ghana have not received much attention in the application of Sm-Nd isotope systematics. Limited data available recorded εNd(t) values ranging from +2.7 to +3.5 for the Kumasi basin granitoids, +2.3 for a localised mafic dike (Losiak et al., 2013) and −0.8 to +1.37 for the Bole-Nangodi belt (Table 4) (Sakyi et al., 2020a). Sakyi et al. (2020a) also reported Nd (T_{DM1}) and Nd (T_{DM2}) model ages of 2.53-2.34 Ga and 2.39-2.21 Ga respectively, for the Bole-Nangodi belt (Table 4), however, the T_{DM2} ages appear to be very consistent and generally close to the 2.1 Ga formation age of the Birimian crust. Similarly, Nd model ages of 2.29-2.17 Ga have been reported for various Birimian plutonic suites, except the ~2.60 Ga age reported for Winneba granitoids (Table 2; Taylor et al., 1992).

4. Discussion

4.1. Petrogenesis

Recent studies of the Paleoproterozoic Birimian granitoids in Ghana have revealed varying source materials and petrogenetic processes. The main components of the crust in the Paleoproterozoic WAC region of Ghana comprise tonalite-trondhjemite-granodiorite (TTG) suites, low-K to high-K calc-alkaline granites, LILE-enriched diorites, high-K quartz monzonites, two-mica granites, and muscovite leucogranites (e.g., Grenholm, 2011; Block et al., 2016b; McFarlane et al., 2019a, 2019b; Sakyi et al., 2020a; Amponsah et al., 2023).

Their derivation from partial melting of metabasaltic to metatonalitic source, with a possible contribution from metagreywacke was proposed by Dampare et al. (2005), whereas the reworking of older felsic crustal rocks and melting of LILE-enriched mantle sources is favoured by Block et al. (2016b). Block et al. (2016b) further explain that, a juvenile mafic proto-crust was extracted from the depleted mantle in an oceanic environment remote from any pre-existing continental nucleus, and was reworked in several primitive magmatic arcs or in an accreted oceanic plateau.

Based on the above assumptions, the granitoids (e.g., the TTGs) have been suggested to have formed by partial melting of hydrous basaltic crust/low-K mafic crust metasomatized chiefly by slab-derived melts at differential depths (e.g., Grenholm, 2011; Anum et al., 2015; Block et al., 2016b; McFarlane et al., 2019b; Sakyi et al., 2020a; Kwayisi et al., unpublished) at pressures where garnet and amphibole were the stable phases (Sakyi et al., 2020a). The formation of the K-rich granitoids is ascribed to the partial melting of the TTGs triggered by subduction-related metasomatism (Losiak et al., 2013; Sakyi et al., 2020a).

Fig. 14a–d are discrimination diagrams to assess the source and petrogenesis of the granitoids. The data show that the samples are silica-rich (mainly >60 wt%), with high Sr/Y and $(La/Yb)_N$ values, and plot

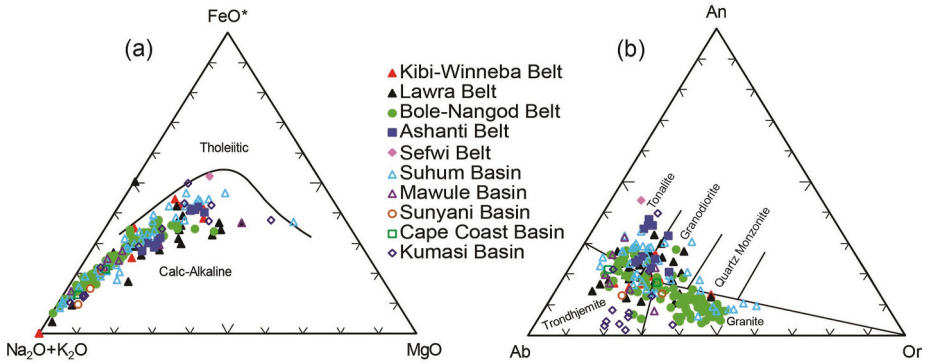

Fig. 6. Classification and discrimination diagrams for the Birimian plutonic rocks of Ghana. (a) AFM (A= K_2O + Na_2O), F= FeO_{tot}, M = MgO) diagram (Irvine and Baragar, 1971), showing a calc-alkaline affinity for the Birimian plutonic rocks; (b) Normative Ab-An-Or classification diagram (O'Connor, 1965). Data sources as in Figs. 3 and 4.

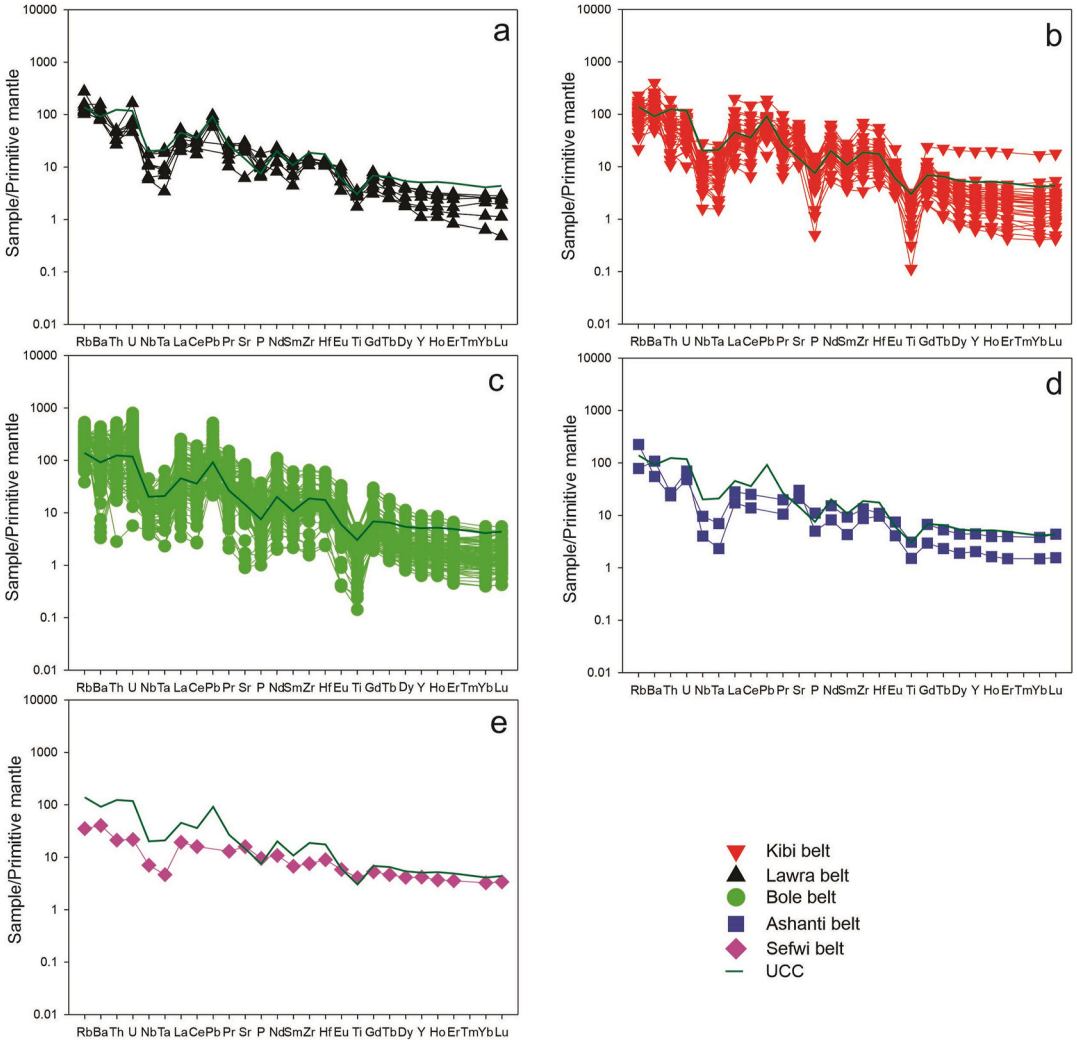

Fig. 7. Primitive mantle-normalized multi-element diagrams for the belt-type granitoids (Normalizing values are from Palme and O'Neill, 2014; UCC values are from Rudnick and Gao, 2003). Data sources as in Figs. 3 and 4.

largely in the adakite field of the Sr/Y vs. Y (Fig. 14a) and $(La/Yb)_N$ vs. Yb_N (Fig. 14b) diagrams. On the SiO_2 vs. MgO plots, granitoids from the Ashanti belt mainly display affinity for metabasaltic and eclogite melts and adakites derived from thickened lower crust (Fig. 14c) whereas majority of the granitoids plot mainly within modern adakites and TTG>3.5 Ga, with other granitoids broadly distributed (Fig. 14d). High Sr/Y and $(La/Yb)_N$, and low HREE (e.g. Yb) are considered as a proxy for dehydration partial melting of metabasalt in the stability field of garnet (e.g., Martin, 1987; Drummond and Defant, 1990; Moyen, 2009). They may, therefore, be classified as high silica adakites. In addition to high Sr/Y, the high SiO_2 and La/Yb values suggest that the granitoids were formed in a thickened lower crust (Aidoo et al., 2021). The occurrence of

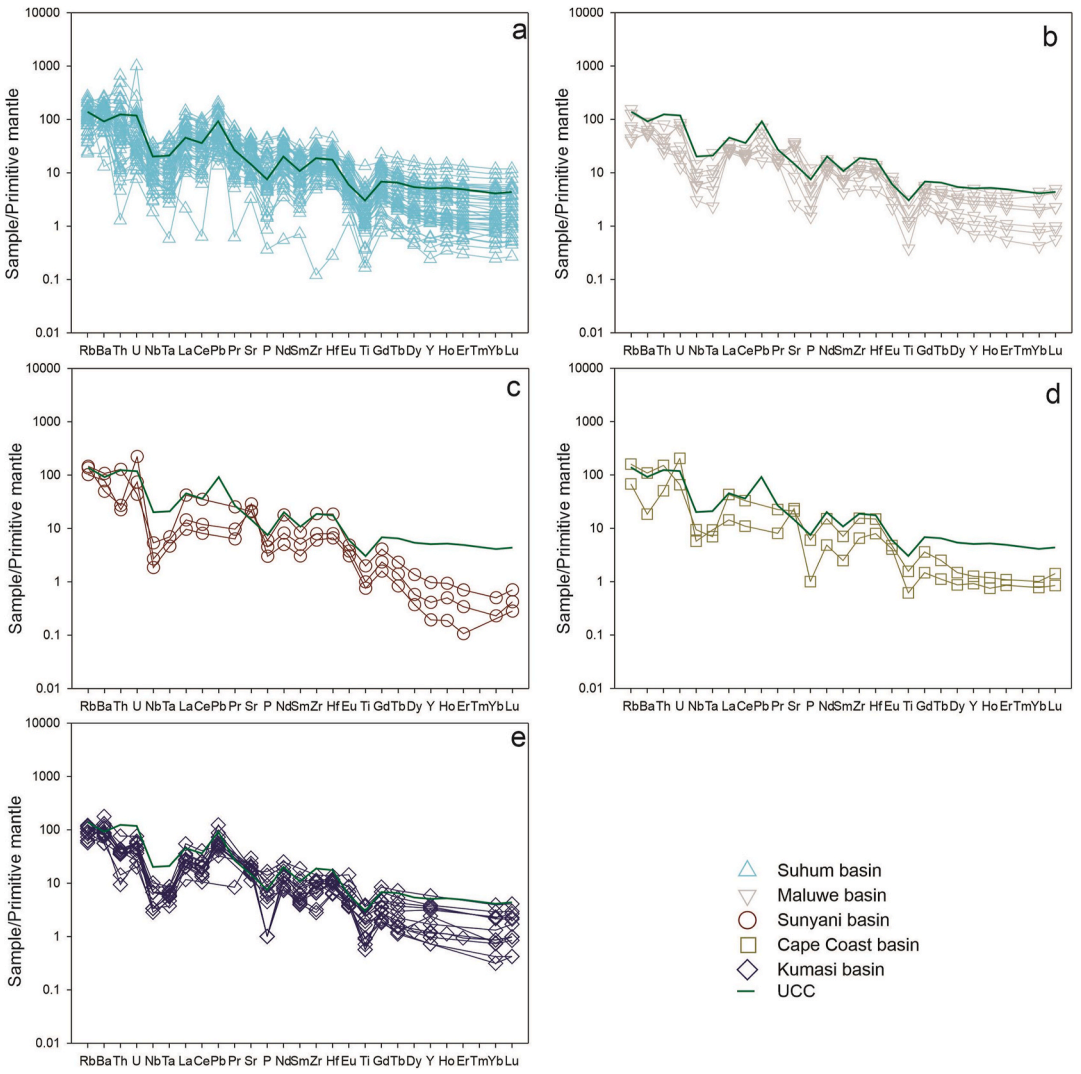

Fig. 8. Primitive mantle-normalized multi-element diagrams for the basin-type granitoids ((Normalizing values are from Palme and O'Neill, 2014; UCC values are from Rudnick and Gao, 2003). Data sources as in Figs. 3 and 4.

mafic enclaves with dioritic to gabbroic compositions in some of the granitoids are interpreted to represent remnants of basic magma (Sakyi et al., 2020a, 2020b), and may be indicative of magma mixing processes (Sakyi et al., 2014, 2020a, 2020b; Anum et al., 2015).

Thermobarometric calculations revealed crystallization temperatures and pressures of 650–685 °C and 4–7 kbar respectively (Kibi-Winneba belt; Dampare et al., 2005), ~640–750 °C and ~2–6 kbar respectively (Bole-Nangodi belt; Sakyi et al., 2020a) and ~632–712 °C and 5.2–7.2 kbar respectively (Suhum basin; Kwayisi et al., unpublished). These relatively low temperatures and pressures range suggest a lower crustal source (Dampare et al., 2005; Losiak et al., 2013; Sakyi et al., 2020a).

4.2. Reworking of older crustal material

Until recently, evidence for reworking of Archean basement during Birimian magmatism in Ghana has been attributed to whole rock Nd model ages of the Winneba pluton and sparse inherited zircon grains from rocks in the Bole-Nangodi belt of northwestern Ghana (Petersson et al., 2016). The Winneba-type granitoids were considered to be the only rock suite in Ghana which showed evidence of a significant magmatic contribution from reworked ancient crust in their genesis, with an Archean sialic precursor ($\varepsilon Nd = -5.3$ and Nd model age of ~2.6 Ga) (Leube et al., 1990; Taylor et al., 1992). Several lines of evidence suggest that the main Paleoproterozoic crustal growth event, also known as the Eburnean orogeny, in the WAC involved a significant juvenile crust-forming process, with little to no involvement of Archean crustal components (e.g., Abouchami et al., 1990; Liégeois et al., 1991; Boher et al., 1992; Taylor et al., 1992; Pawlig et al., 2006). However, studies have suggested that the magmas that generated the Birimian terrane were likely derived from source(s) containing recycled materials. This is based on evidence from the εHf, εNd, and model ages of granitoids, metavolcanic, and metasedimentary rocks (e.g., Sakyi et al., 2018; Amponsah et al., 2023). In this review, we focused on the granitoid plutons.

Evolved crustal signatures are those with relatively low εHf values while juvenile rocks input shows high εHf values close to that of depleted mantle (e.g., Dhuime et al., 2012; Roberts, 2012; Gardiner et al., 2016; Ustaömer et al., 2016; Azzouni-Sekkal et al., 2020; Matos et al., 2023). Thus, granitoids displaying high values of $\varepsilon Hf_{(t)} \gg 0$ represent juvenile mantle input, either directly via mantle-derived mafic melts or by remelting of a young mantle-derived mafic lower crust (Kröner et al., 2013). On the other hand, εHf values $\ll 0$ indicate evidence of melting of old continental crust, whereas $\varepsilon Hf_{(t)}$ values around zero indicate the mixing of old crust and depleted mantle-derived material during their formation.

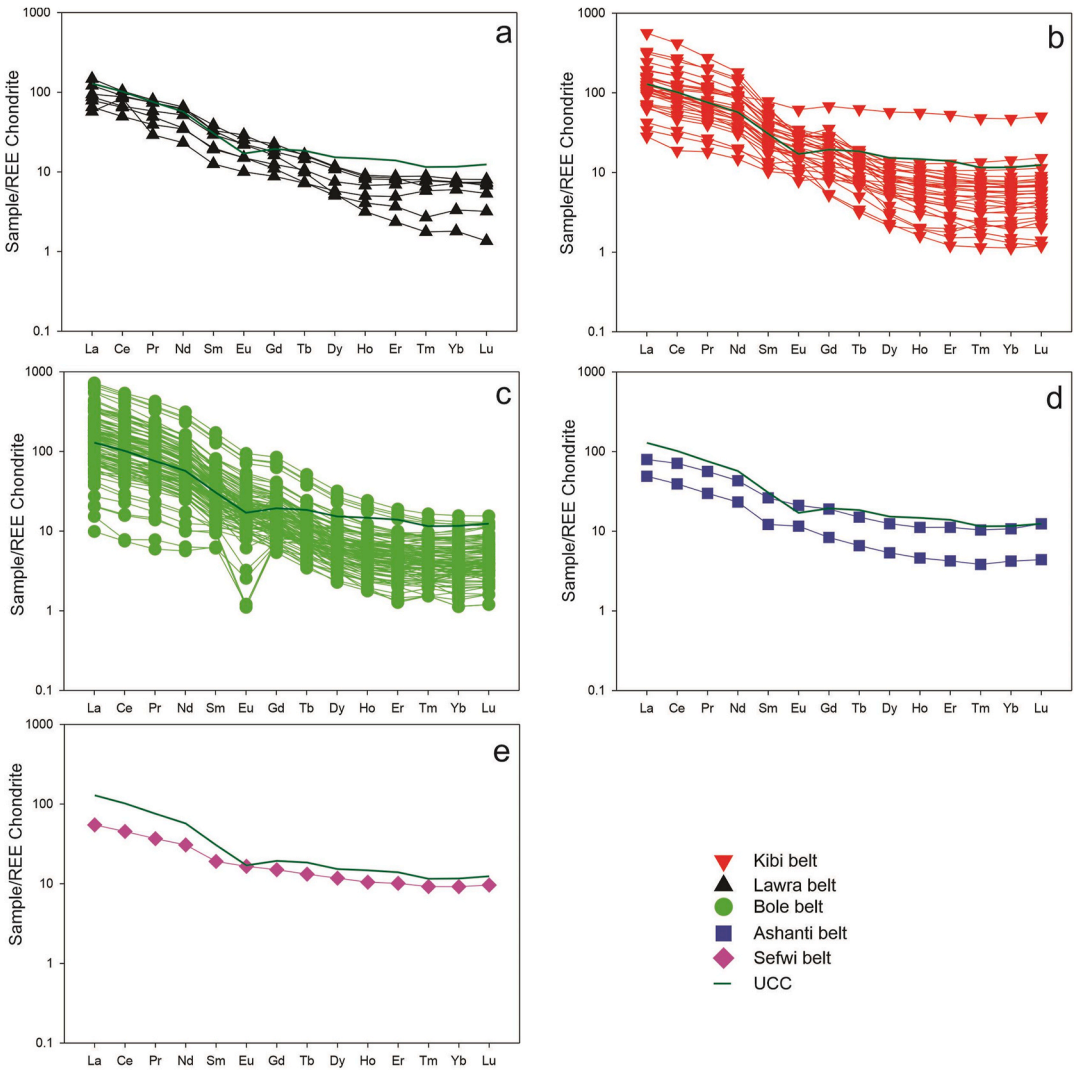

Fig. 9. Chondrite-normalized REE diagrams for the belt-type granitoids (Chondrite values are from Palme and O'Neill, 2014). Data sources as in Figs. 3 and 4.

The compiled εHf values of −14.5 to +7.6 (Table 3, S3; Fig. 12a) and εNd values (Table 4, Fig. 15) strongly indicate that reworking of older crustal material was a common phenomenon in the genesis of the parental magmas of the granitoids. The positive $\varepsilon Hf_{(t)}$ values of up to +7.6 indicate that the zircons crystallized from juvenile liquids derived from a depleted mantle with little or no crustal contamination, whereas the negative $\varepsilon Hf_{(t)}$ values, up to −14.5 indicate minor to significant involvement of older crustal material, possibly Archean.

Block et al. (2016b) explained that the supra-chondritic Hf isotope compositions indicate that the granitoids were derived from the reworking of juvenile crustal components. In contrast, granitic plutons in the Ashanti belt probably formed via either juvenile addition from the mantle or reworking of only slightly older crust (Oberthür et al., 1998). Likewise, de Kock et al. (2011) attributed the presence of older cores and grains in younger rocks in the Wa-Bole enclave to the continuous reworking of the developing crust during successive magmatic episodes with discordant cores in zircon suggesting the presence of Archean material in the Paleoproterozoic source rocks in the study region. Combined U-Pb ages of ca. 2229-2092 Ma and εHf data of −10.9 to +6.3 suggest juvenile crustal addition with reworking of Archean crust (Petersson et al., 2016). Likewise, the reworking of Archean crust recorded in zircons from both northwestern and southeastern Ghana has been explained by sub-chondritic εHf values of −10.5 to +4.4 of the zircons (Petersson et al., 2018). The minimum εHf value of −10.5 (at 2139 Ma) suggests a Palaeoarchaean to late Mesoarchaean component as the contributing older source (Petersson et al., 2018). This is further affirmed by Amponsah et al. (2023), who explained that the model ages (T_{DM2}) of 2789-2456 Ma and εHf values of −1.5 to +5.4 for granitoids in the Suhum basin indicate the magmas were sourced from the early Paleoproterozoic juvenile mantle with substantial Neoarchean crustal component.

In the Bole-Nangodi belt of northern Ghana, the εNd values of −0.86 to +1.37 with T_{DM1} ages of 2.34–2.53 Ga and T_{DM2} ages of 2.21–2.39 Ga (Fig. 15) for the granitoids indicate their juvenile character, possibly a depleted mantle source with minor contributions from a pre-Birimian (or Archean?) crustal material in their source material(s) (Sakyi et al., 2020a). The positive $\varepsilon Nd_{(t)}$ values between +2.8 and + 3.5 for Kumasi basin granitoids and their proximity to the depleted mantle array (Fig. 15) indicate short crustal residence times of the magma, meaning that the granitoids were derived from a juvenile mantle protolith during the Paleoproterozoic without significant admixture of an Archean crustal component (Losiak et al., 2013). Similarly, the whole-rock Nd isotope model age of ca. 2.6 Ga for the Winneba showed evidence for a significant magmatic contribution from reworked ancient crust in their genesis, with an Archean sialic precursor (Leube et al., 1990; Taylor et al., 1992).

Available Hf and Nd data suggest that the identified Archean signature extends beyond the Winneba pluton to the Suhum basin

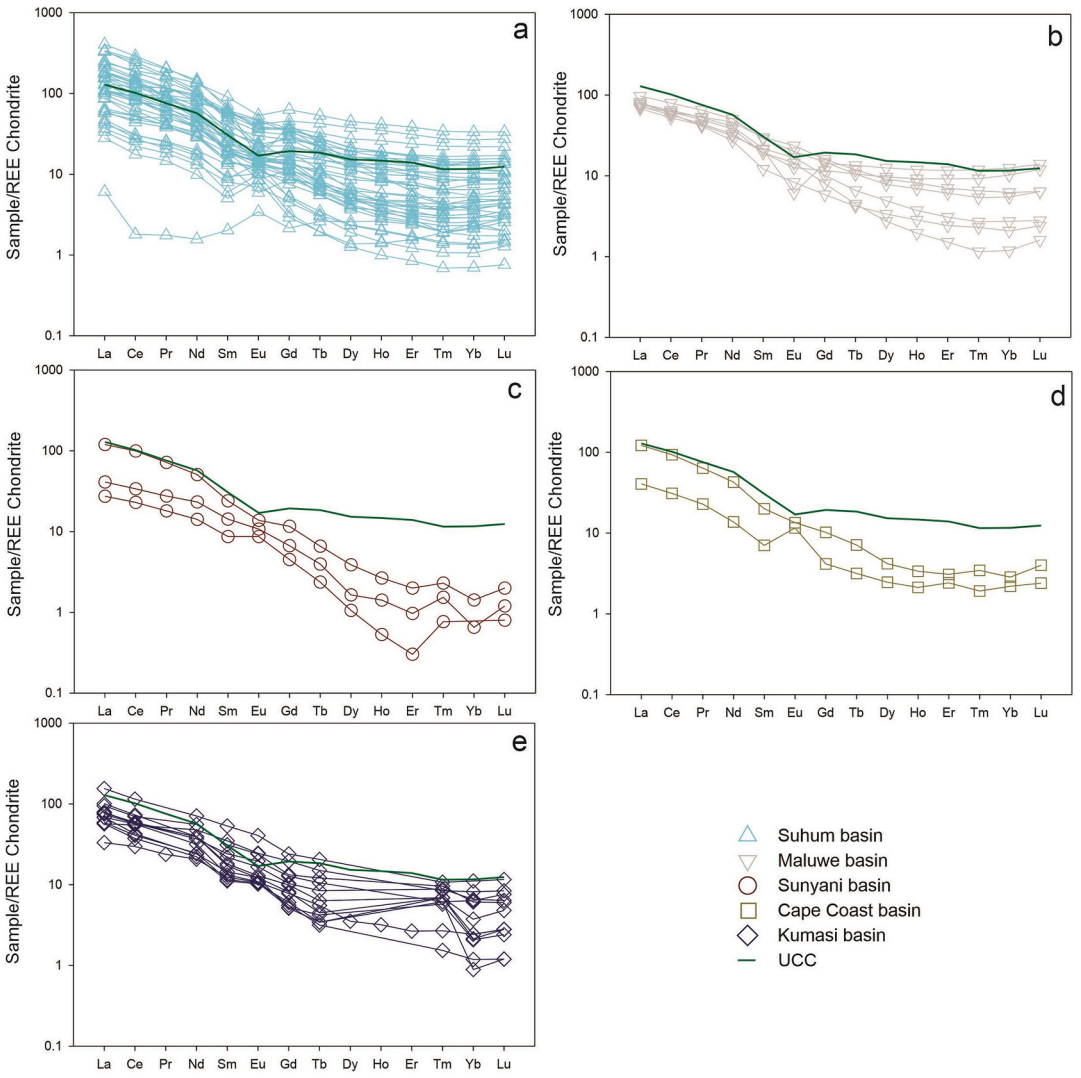

Fig. 10. Chondrite-normalized REE diagrams for the basin-type granitoids (Chondrite values are from Palme and O'Neill, 2014). Data sources as in Figs. 3 and 4.

(Petersson et al., 2016; Amponsah et al., 2023), Kibi-Winneba belt (Petersson et al., 2016), the Nangodi belt (Sakyi et al., 2020a; Nunoo et al., 2022), and on a very minor scale, the Ashanti belt (Parra-Avila et al., 2018). Thus, reworking of Archean crust is not an isolated phenomenon restricted to the Winneba pluton but widespread across the Birimian terrane in Ghana and involved mainly Mesoarchean and Neoarchean crust. Therefore, contrary to the rare inherited older ages reported in the Sefwi belt (McFarlane, 2018), studies have shown that inherited older zircon grains, interpreted to represent Archean zircon cores, are a widespread feature in the Baoulé-Mossi domain of the WAC, of which the Birimian granitoids of Ghana form a part (Petersson et al., 2016; Parra-Avila et al., 2017; de Kock et al., 2011; Nunoo et al., 2022; Amponsah et al., 2023). This phenomenon occurs, notwithstanding the common belief that the Birimian terrane consists of predominantly juvenile crust.

Available data (Fig. 12b), show that the Birimian domains in western and southwestern Ghana largely display radiogenic (juvenile) Hf signatures, except the Ashanti belt which records negative $\varepsilon Hf_{(t)}$ values up to −5.3. The general lack of sub-chondritic εHf signatures in the basins suggests that the basins received more mantle-derived materials through decompression melting, compared to the belts. This contrasts the sub-chondritic signatures in the Bole-Nangodi belt, Kibi-Winneba belt and the Suhum basin, which are dominated by high negative $\varepsilon Hf_{(t)}$ values, up to −14.5. In the Bole-Nangodi belt, the moderate to high negative $\varepsilon Hf_{(t)}$ values (−14.5 to −2.3) are recorded in the northeastern end of the belt (northeastern Ghana; Figs. 2 and 12b). This observation is also made in the southeastern part of Ghana, where both the Kibi-Winneba belt and Suhum basin record high negative $\varepsilon Hf_{(t)}$ values of up to −10.5 and −10.9, respectively (Figs. 2 and 12b). These signatures provide a strong indication that these domains may have close proximity to older crustal materials. Aidoo et al. (2020, 2021) have proposed the existence of an Archean crust along the eastern margin of the WAC and further provided evidence to support the partial melting of Neoarchean lower crust in the formation of the basement rocks of the Pan-African Dahomeyide Belt that lies immediately to the east of the Suhum basin. This corroborates earlier suggestions that isotopic signatures displayed by magmatic rocks in southern Ghana require an Archean crustal source underlying the southeastern part of the Baoule-Mossi domain (Taylor et al., 1992; Petersson et al., 2018; McFarlane et al., 2019b). Therefore, the spatial variation in εHf data indicating predominantly sub-chondritic values towards the southeastern and northeastern part of Ghana, juxtaposed with calculated Hf model ages, strongly give credence to the existence of Neoarchean to Mesoarchean crustal material in eastern Ghana during the Birimian crust formation.

4.3. Geotectonic setting

The geodynamic setting of the Birimian rocks has been investigated

Table 1
Summary of published ages of granitoids in the Paleoproterozoic Birimian terrane of Ghana.

Birimian Domain	Rock Type	Mineral Analysed	Age (Ma)	Method	Reference
Lawra, Bole-Nangodi Belts	Migmatitic gneiss, schist, granofels	Monazite	2141 ± 6–2127 ± 7	U-Pb	Block et al. (2015)
Lawra, Bole-Nangodi Belts	Paragneiss	Monazite	2128 ± 8–2123 ± 8	U-Pb	Block et al. (2016a)
Lawra, Bole-Nangodi Belts	Gneiss, paragneiss	Zircon	2160 ± 28–2111 ± 7	U-Pb	Block et al. (2016a)
Lawra, Bole-Nangodi Belts	Granite, granodiorite, trondhjemite, granodiorite gneiss	Zircon	2211 ± 6–2133 ± 6	U-Pb	Block et al. (2016b)
Bole-Nangodi Belt; Mawule Basin	Granite, granodiorite, gneissic granite, syenite, rhyodacite	Zircon	2195 ± 4–2118 ± 3	U-Pb	de Kock et al. (2011)
Ashanti Belt	Granodiorite, aplite	Zircon	2105±3–2086 ± 4	Pb-Pb	Oberthür et al. (1998)
Ashanti Belt	Granodiorite, aplite	Titanite	2104 ± 2–2092 ± 3	Pb-Pb	Oberthür et al. (1998)
Ashanti Belt	Granitoid	Monazite	2174 ± 2–2105 ± 5	Pb-Pb	Oberthür et al. (1998)
Ashanti Belt	Granitoid	Rutile/galena	2123 ± 2–2106 ± 2	Pb-Pb	Oberthür et al. (1998)
Suhum, Cape Coast, Sunyani Basins	Biotite-hornblende tonalite, Biotite-hornblende granite, Biotite-hornblende granodiorite, two-mica granite, two-mica granodiorite, pegmatite	Zircon	2229 ± 4–2092 ± 4	U-Pb	Petersson et al. (2016)
Kibi-Winneba, Bole-Nangodi, Sefwi Belts/Mawule Basin (1 sample)	Biotite-hornblende granite, biotite granite, granite, two-mica granodiorite, granitic gneiss	Zircon	2219 ± 6–2120 ± 6	U-Pb	Petersson et al. (2018)
Bole-Nangodi Belt	Tonalite, trondhjemite, granodiorite	Zircon	2228 ± 22–2115 ± 4	U-Pb	Nunoo et al. (2022)
Sunyani Basin	Gneiss, paragneiss	Zircon	2073 ± 6–2073 ± 2	U-Pb	McFarlane (2018)
Sefwi Belt	Trondhjemite, quartz diorite, quartz monzonite	Zircon	2159 ± 8–2135 ± 7	U-Pb	McFarlane et al. (2019b)
Suhum Basin	Amphibole-bearing gneiss, biotite gneiss, migmatitic gneiss, leucogranite, gabbro	Zircon	2224 ± 26–2085 ± 110	U-Pb	Amponsah et al. (2023)
Lawra Belt	Hornblende granodiorite, gneissic biotite granite, two-mica granite, biotite granite, Pyroxene-hornblende gneiss	Zircon	2213 ± 76–2131 ± 10	U-Pb	Sakyi et al. (2014)
Kibi-Winneba Belt	Hornblende granodiorite, biotite granodiorite, gneissic biotite granite	Zircon	2193 ± 9–2127 ± 7	U-Pb	Anum et al. (2015)
Bole-Nangodi Belt	Hornblende granite, two-mica granite, granodiorite,	Zircon	2181 ± 94–2074 ± 49	U-Pb	Sakyi et al. (In Review)
Kumasi Basin	Granite, muscovite granite, two-mica granite	Zircon	2098 ± 6–2092 ± 6	U-Pb	Losiak et al. (2013)
Ashanti Belt	Granite, granodiorite	Zircon	2191 ± 6–2157 ± 5	U-Pb	Parra-Avila et al. (2015)
Ashanti Belt	Granite	Zircon	2125 ± 20–2058 ± 22	U-Pb	Parra-Avila et al. (2018)
Kibi-Winneba, Ashanti, Sefwi Belts	Biotite-hornblende tonalite, biotite granite,	Zircon	2232 ± 5–2169 ± 13	U-Pb	Grenholm (2011)
Suhum, Sunyani, Cape Coast Basins	Biotite-hornblende granodiorite, biotite-hornblende granite, two-mica granodiorite,	Zircon	2180 ± 4–2090 ± 60	U-Pb	Grenholm (2011)
Sefwi, Kibi-Winneba Belts	Granodiorite, monzonite, metadiorite,	Zircon	2222 ± 32–2159 ± 4	Pb-Pb	Feybesse et al. (2006)
Suhum Basin	Amphibolite, gabbro	Amphibole	2095 ± 34–1978 ± 37	K-Ar	Feybesse et al. (2006)
Kibi-Winneba Belt	Granite, pegmatite	Biotite/ Muscovite	2019 ± 14–1907 ± 14	K-Ar	Chalokwu et al. (1997)
Ashanti, Sefwi Belts	Granitoids	Zircon	2179 ± 2–2172 ± 2	Pb-Pb	Hirdes et al. (1992)
Sunyani, Kumasi Basins	Muscovite granite, biotite tonalite	Zircon	2116 ± 2–2088 ± 1	Pb-Pb	Hirdes et al. (1992)
Kumasi Basin	Granite, granodiorite, diorite	Zircon	2136 ± 9–2090 ± 44	U-Pb	Adadey et al. (2009)
Kibi-Winneba, Ashanti Belts	Granite, pegmatite	Zircon	2132 ± 4–2080 ± 3	U-Pb	Agyei-Duodu et al. (2009)
Suhum, Cape Coast, Sunyani Basins	Granodiorite, granite, granitic gneiss	Zircon	2187 ± 1–2072 ± 1	U-Pb	Agyei-Duodu et al. (2009)
Sefwi Belt	Rhyolite	Zircon	2189 ± 1	U-Pb	Hirdes and Davis (1998)

by many researchers who hold different views. On the one hand the Birimian juvenile crust was produced in subduction-related magmatism in arc environments (e.g., Mortimer, 1992; Sylvester and Attoh, 1992; Pohl and Carlson, 1993; Asiedu et al., 2004; Dampare et al., 2005, 2008; Baratoux et al., 2011; Senyah et al., 2016). This hypothesis describes the assemblage of oceanic island arcs during subduction processes. On the other hand, the Birimian juvenile crust may have been generated from plume-related magmatism (e.g., Abouchami et al., 1990; Boher et al., 1992; Lompo, 2009). The mantle plume-related magmatism favours rapid crustal growth, subsequent formation of extensive oceanic

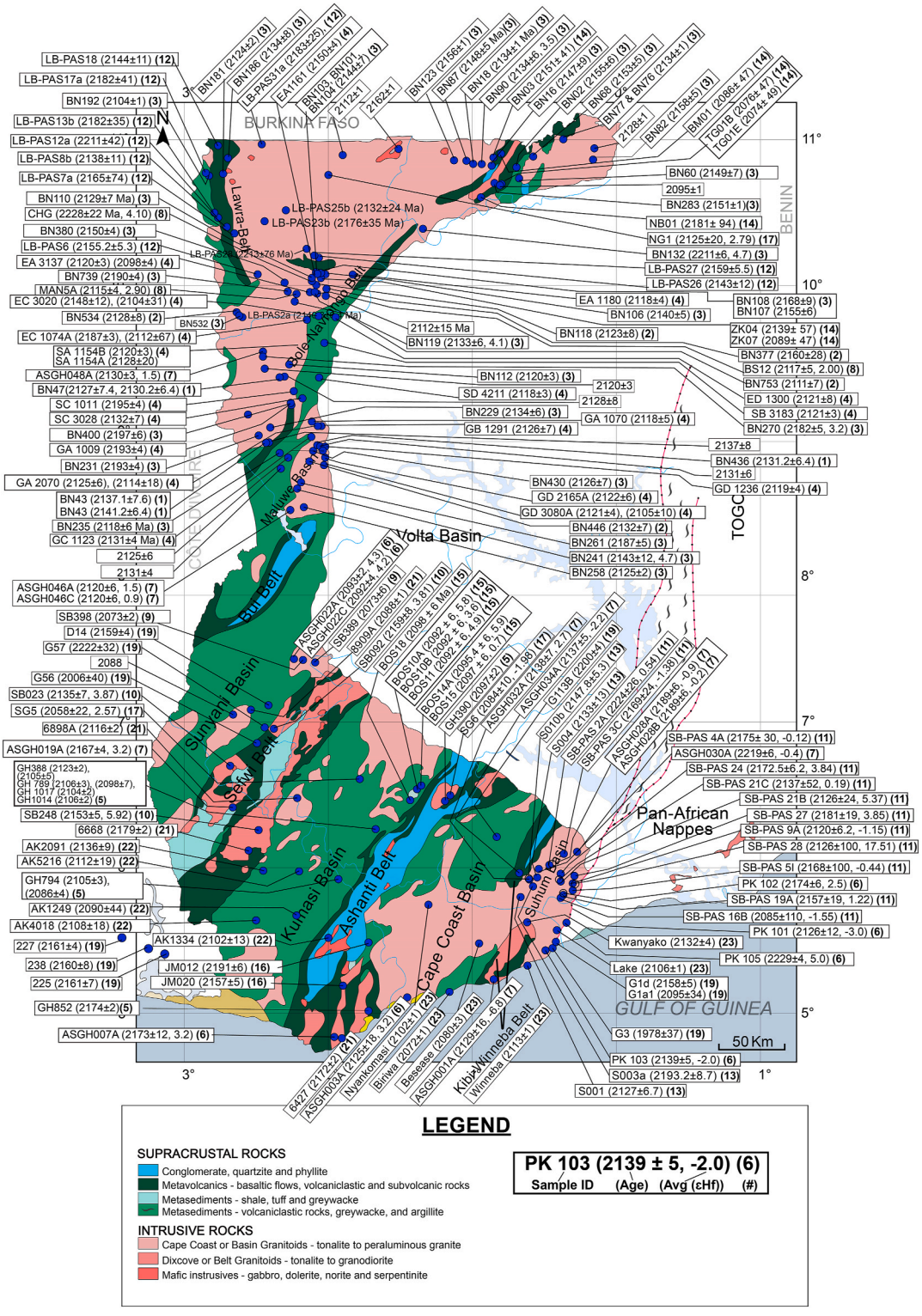

Fig. 11. Geological map of the Birimian terrane of Ghana (modified after Petersson et al., 2016) showing locations of dated granitoids compiled from the literature. Data References: 1 - Block et al. (2015); 2 - Block et al. (2016a); 3 - Block et al. (2016b); 4 - de Kock et al. (2011); 5 - Oberthür et al. (1998); 6 - Petersson et al. (2016); 7 - Petersson et al. (2018); 8 - Nunoo et al. (2022); 9 - McFarlane (2018); 10 - McFarlane et al. (2019b); 11 - Amponsah et al. (2023); 12 - Sakyi et al. (2014); 13 - Anum et al. (2015); 14 – Sakyi et al. (In Review); 15 - Losiak et al. (2013); 16 - Parra-Avila et al. (2015); 17 - Parra-Avila et al. (2018); 18 - Grenholm (2011); 19 - Feybesse et al. (2006); 20 - Chalokwu et al. (1997); 21 - Hirdes et al. (1992); 22 - Adadey et al. (2009); 23 - Agyei-Duodu et al. (2009); 24 - Hirdes and Davis, 1998.

plateaus and initiation of intra-oceanic subduction as the plateaus collided with each other or with micro-continental fragments. Based on the hypotheses, two models have been proposed to account for the tectonic processes involved in the formation of the rocks: (i) accretionary orogeny which supports the subduction-related magmatism (e.g., Boher et al., 1992; Davis et al., 1994; Feybesse and Milési, 1994; Hirdes et al., 1996; Ledru et al., 1994; Hirdes and Davis, 2002), and (ii) the transcurrent tectonics models, supporting the plume

Table 2
Whole-rock Rb-Sr and Pb-Pb isochron ages and Nd and Hf model ages for Birimian granitoids in Ghana.

Rock Suite	Rb-Sr Age (Ma)	Pb-Pb Age (Ma)	Nd Model Age TDM (Ga)	Hf Model Age	Reference
Upper West granitoids	2086 ± 40	2095	2.19 - 2.20 Ga	–	Taylor et al. (1992)
Kumasi granitoids	2127 ± 65	2114	2.17 Ga	–	"
Dixcove granitoids	1891 ± 314	2061	2.20 - 2.24 Ga	–	"
Cape Coast granitoids	2216 ± 72	1973	2.24 - 2.29 Ga	–	"
Winneba granitoids	2024 ± 159	2173	2.59 - 2.60 Ga	–	"
Bole-Nangodi Belt	–	–	2.21–2.53 Ga	–	Sakyi et al. (2020a)
Sefwi Belt	–	–	–	2.26 - 2.64 Ga	McFarlane et al. (2019b)
Different Locations	–	–	–	2.4 - 3.1 Ga	Parra-Avila et al. (2018)
Bole-Nangodi Belt	–	–	–	2.35-2.61 Ga	Block et al. (2016b)
Suhum Basin	–	–	–	2789 - 2456 Ma	Amponsah et al. (2023)
Bole-Nangodi Belt	–	–	–	2250 - 2571 Ma	Nunoo et al. (2022)
Different Locations	–	–	–	3230 - 2780 Ma	Petersson et al. (2018)
Different Locations	–	–	–	2688 - 2175 Ma	Petersson et al. (2016)

magmatism (e.g., Bassot, 1987; Doumbia et al., 1998; Pouclet et al., 1996). However, recent studies on the Paleoproterozoic rocks in the Birimian terrane of the WAC have produced avenues for challenging discussions concerning the various models for the geodynamic evolution of these rocks. For example, studies have also shown that the juvenile crust of southwest Ghana was generated in an intraoceanic arc setting, associated with diverse and intense subduction-related magmatism until subsequent terrane accretion and collision (McFarlane, 2018). Similarly, the formation and accretion of the West African Craton reflect the amalgamation of individual oceanic arc terranes, through episodic collisional orogenesis (McFarlane et al., 2019a, 2019b), providing further support for an accretionary tectonic evolution under an arc-type setting that later evolved into a collisional-type setting. Parra-Avila et al. (2018) hypothesized that the Baoulé-Mossi domain of the southern WAC formed through accretion of the arc systems, subsequently evolving into a collisional orogeny when the amalgamated arcs were indented by the Archean Kénéma-Man domain (Parra-Avila et al., 2018). This hypothesis is akin to that of Parra-Avila et al. (2017, 2019), that suggested the evolution of the Paleoproterozoic portion of the southern WAC in a compressional-type environment through the amalgamation of at least two crustal blocks that indicate an evolution from magmatic accretion/crustal growth to crustal reworking. These hypotheses from recent studies generally favour the accretion of several oceanic arcs.

The geochemical data derived from studies conducted on Birimian granitoids in Ghana so far display similar characteristics and trends. They exhibit volcanic arc granites (VAG) and syn-collisional (Syn-COLG) granites signatures (Fig. 16a and b), and also show calc-alkaline signatures, enrichment of LILE and LREE and depletion of HFSE and HREE, with slight negative to positive Eu and Sr anomalies. Typically, the granitoids display enrichment in Ba, Th, and Pb, and depletion in Nb-Ta, T and P, and low Nb/Th ratios (Figs. 7–10). These distinctive geochemical signatures are considered important indicators of arc-type environments dominated by subduction processes (Arculus et al., 1999; Hawkesworth and Kemp, 2006; Hofmann, 1997; Moyen and Martin,

Table 3
Average εHf(t) and corresponding U-Pb data for Birimian granitoids of Ghana.

Sample	Rock type	Age (Ma)	Avg. (εHf)	±2σ (mean)	Reference
BN 119	Granite	2133 ± 6	+4.1	1.3	Block et al. (2016b)
BN 132	Granite gneiss	2211 ± 6	+4.7	1.4	Block et al. (2016b)
BN 270	Granodiorite gneiss	2181 ± 5	+3.2	1.2	Block et al. (2016b)
BN 241	Trondhjemite	2143 ± 12	+4.7	1.5	Block et al. (2016b)
BN 90	Granite	2135 ± 6	+3.5	1.2	Block et al. (2016b)
PK101	Biotite hornblende tonalite	2126 ± 12	−3.0	1.0	Petersson et al. (2016)
PK102	Biotite hornblende granite	2174 ± 6	+2.5	5.1	Petersson et al. (2016)
PK103	Biotite hornblende granite	2139 ± 5	−2.0	1.1	Petersson et al. (2016)
PK105	Biotite hornblende granodiorite	2229 ± 4	+5.0	0.9	Petersson et al. (2016)
ASGH003A	Two-mica granodiorite	2125 ± 18	+3.2	1.2	Petersson et al. (2016)
ASGH007A	Hornblende tonalite	2173 ± 12	+3.2	1.0	Petersson et al. (2016)
ASGH022A	Mica granite	2093 ± 2	+4.3	1.1	Petersson et al. (2016)
ASGH022C	Mica granite	2092 ± 4	+4.2	0.9	Petersson et al. (2016)
ASGH001A	Granite	2129 ± 16	−6.8	1.4	Petersson et al. (2018)
ASGH019A	Biotite hornblende granite	2167 ± 4	+3.2	1.1	Petersson et al. (2018)
ASGH028A	Biotite hornblende granite	2189 ± 6	−0.9	1.0	Petersson et al. (2018)
ASGH028B	Biotite hornblende granite	2189 ± 6	−0.2	1.0	Petersson et al. (2018)
ASGH030A	Biotite hornblende granite	2219 ± 6	−0.4	1.0	Petersson et al. (2018)
ASGH032A	Biotite hornblende granite	2129 ± 14	+2.7	1.3	Petersson et al. (2018)
ASGH034A	Biotite hornblende granite	2137 ± 5	−2.2	1.0	Petersson et al. (2018)
ASGH046A	Two-mica granodiorite	2120 ± 6	+1.5	0.9	Petersson et al. (2018)
ASGH046C	Two-mica granodiorite	2120 ± 6	+0.9	1.2	Petersson et al. (2018)
ASGH047A	Granitic gneiss	2204 ± 4	+0.9	1.0	Petersson et al. (2018)
ASGH048A	Biotite granite	2130 ± 3	+1.5	1.1	Petersson et al. (2018)
BOS10A	Muscovite granite	2092 ± 6	+5.8	–	Losiak et al. (2013)
BOS10B	Muscovite granite	*2092* ± *6*	+3.6	–	Losiak et al. (2013)
BOS11	Muscovite granite	*2092* ± *6*	+4.9	–	Losiak et al. (2013)
BOS14A	Muscovite granite	2095 ± 6	+5.9	–	Losiak et al. (2013)
BOS15	Muscovite granite	2097 ± 6	+0.7	–	Losiak et al. (2013)
NG1	Granite	2125 ± 20	+2.8	1.0	Parra-Avila et al. (2018)
SG5	Granitic intrusion	2058 ± 22	+3.6	0.9	Parra-Avila et al. (2018)

(*continued on next page*)

Table 3 (*continued*)

Sample	Rock type	Age (Ma)	Avg. (εHf)	±2σ (mean)	Reference
SG6	Granitic intrusion	2084 ± 10	−2.0	1.0	Parra-Avila et al. (2018)
SB248	Foliated biotite trondhjemite	2153 ± 5	+5.9	1.0	McFarlane et al. (2019b)
SB092	Hornblende quartz diorite	2159 ± 8	+3.8	1.2	McFarlane et al. (2019b)
SB023	Quartz monzonite	2135 ± 7	+3.9	1.0	McFarlane et al. (2019b)
CHG	Granodiorite	2228 ± 22	+4.1	0.3	Nunoo et al. (2022)
BS12	Trondhjemite	2117 ± 5	+2.0	0.9	Nunoo et al. (2022)
MAN 5A	Tonalite	2115 ± 4	+2.9	0.9	Nunoo et al. (2022)
SB-PAS 2A	Amphibole-bearing gneiss	2224 ± 26	+0.5	–	Amponsah et al. (2023)
SB-PAS 3C	Amphibole-bearing gneiss	2169 ± 24	−1.4	–	Amponsah et al. (2023)
SB-PAS 4A	Biotite gneiss	2175 ± 30	−0.1	–	Amponsah et al. (2023)
SB-PAS 5I	Amphibole-bearing gneiss	2168 ± 100	−0.4	–	Amponsah et al. (2023)
SB-PAS 9A	Migmatitic gneiss	2120 ± 6	−1.1	–	Amponsah et al. (2023)
SB-PAS 16B	Intrusive leucogranite	2085 ± 110	−1.5	–	Amponsah et al. (2023)
SB-PAS 19A	Amphibole-bearing gneiss	2157 ± 19	+1.2	–	Amponsah et al. (2023)
SB-PAS 21B	Intrusive leucogranite	2126 ± 24	+5.4	–	Amponsah et al. (2023)
SB-PAS 21C	Amphibole-bearing gneiss	2137 ± 52	+0.2	–	Amponsah et al. (2023)
SB-PAS 24	Amphibole-bearing gneiss	2173 ± 6	+3.8	–	Amponsah et al. (2023)
SB-PAS 27	Migmatitic gneiss	2181 ± 19	+3.8	–	Amponsah et al. (2023)

[#] Amponsah et al. (2023) reported whole-rock data.

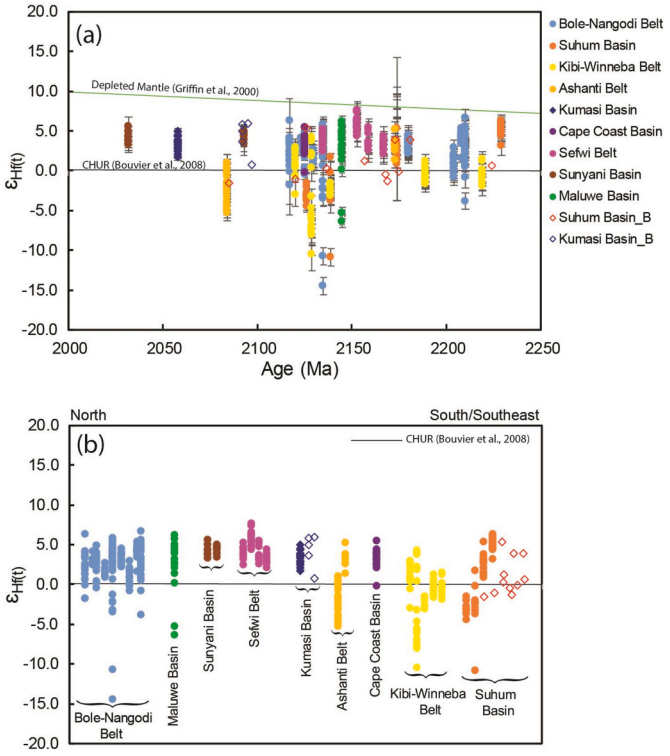

Fig. 12. εHf vs. crystallization ages of the granitoid plutons. Ages represent interpreted igneous crystallization ages for individual samples. Data sources; Losiak et al. (2013); Block et al. (2016b); Petersson et al. (2016, 2018); Parra-Avila et al. (2018); McFarlane et al. (2019b); Nunoo et al. (2022); Amponsah et al. (2023). Each data point represents a single zircon with an assigned U-Pb age. Exceptions are Kumasi Basin_B (average values; Losiak et al., 2013) and Suhum Basin_B (whole-rock data; Amponsah et al. (2023). CHUR data is from Griffin et al. (2000) and Depleted Mantle data is from Bouvier et al. (2008)

2012; Rudnick and Gao, 2003; Zheng, 2019), but they also can be the result of crustal contamination and/or intra-crustal melting (Parra-Avila et al., 2019).

The LREE and LILE enrichment are common indicators of the influence of subduction-related fluids during melting process, whereas the depletion of HREE and positive to negative anomalies displayed by Sr and Eu are characteristics of an evolved magma source with varying degrees of fractionation of plagioclase + hornblende + pyroxene (Sakyi et al., 2014; Anum et al., 2015; Abitty et al., 2016) or indicating that garnet was a stable phase in the source region (Grenholm, 2011). This is because fluid-mobile elements such as LILE, Pb, LREE and Th are insoluble in water but soluble in hydrous silicate melts (e.g., Kogiso et al., 1997; Kessel et al., 2005), whereas fluid-immobile HFSE such as Nb, Ta, Ti, Zr and Hf, and also HREE are usually viewed as immobile in subduction zone fluids (e.g., Tatsumi et al., 1986; Brenan et al., 1994, 1995; Keppler, 1996). Zr-Hf is highly insoluble in hydrous fluids, resulting in negative anomalies of Zr-Hf in typical arc volcanic rocks (Liu et al., 2023). Therefore, the positive Zr-Hf was likely derived from slab-derived melts rather than fluids, whereas the depletion in Nb, Ta, and Ti indicates that hornblende and/or Fe–Ti oxides (e.g., rutile and ilmenite) are residual minerals (Zhang et al., 2022).

Thus, mantle sources of magma relatively depleted in HFSE but enriched in Pb, result in negative Nb-Ta anomalies but a positive Pb anomaly in arc magmas. Thus, the Birimian granitoids are interpreted to have formed in an arc setting (subduction zone), where the enrichment of the LREE and LILE indicates the influence of subduction-related fluids during the melting process in a volcanic arc region, whereas LREE depleted curves indicate sources without fluid enrichment (Anum et al., 2015). The negative to positive Eu and Sr anomalies indicate evolved magma source with varying degrees of fractionation of plagioclase + hornblende + pyroxene, and further suggests evolution of a juvenile crust (Sakyi et al., 2014, 2020a). These features, coupled with their calc-alkaline signatures with Ba, Th and Pb enrichment, positive Zr-Hf, and pronounced Nb-Ta-P-Ti troughs exhibited by the granitoids are typical characteristics of subduction-related magmas, with possible interaction of slab-derived melts (Sakyi et al., 2014, 2020a; Anum et al., 2015), and with minor crustal contamination/assimilation (Abitty et al., 2016; McFarlane et al., 2019b). The shoshonitic affinity displayed by granitoids from the Suhum basin and the Bole-Nangodi belt indicates their emplacement in arc and post-collision settings following an episode of crustal thickening (e.g., Laurent et al., 2014; Lu et al., 2015; Eglinger et al., 2017; Luo et al., 2017).

Generally, the geochemical data are consistent with, and have firmly established an arc tectonic setting arising from subduction-accretion processes. The WAC is proposed to represent the ancient expression of a subduction-collision system, with intermediate characteristics of late Archean and Phanerozoic accretionary orogenic systems (e.g., Parra-Avila et al., 2018; McFarlane et al., 2019b; Sakyi et al., 2020a). However, existing studies on the Birimian plutons in southeastern WAC hardly explains whether the arc environment is oceanic or continental. Few studies have proposed an arc-back-arc basin development along an extensive intraoceanic volcanic-arc system (e.g., de Kock et al., 2011, 2012; Anum et al., 2015; Abitty et al., 2016) and crustal anatexis during an oceanic arc-arc collisional event (McFarlane et al., 2019b). In this review, the geochemical data plot almost exclusively in fields defined by continental arc (Fig. 16c–e), thus strongly establishing a continental arc setting for the Birimian granitoids formed.

The evolution of the Birimian volcanic belts and basins in southeastern WAC can be explained using the tectonic model proposed in

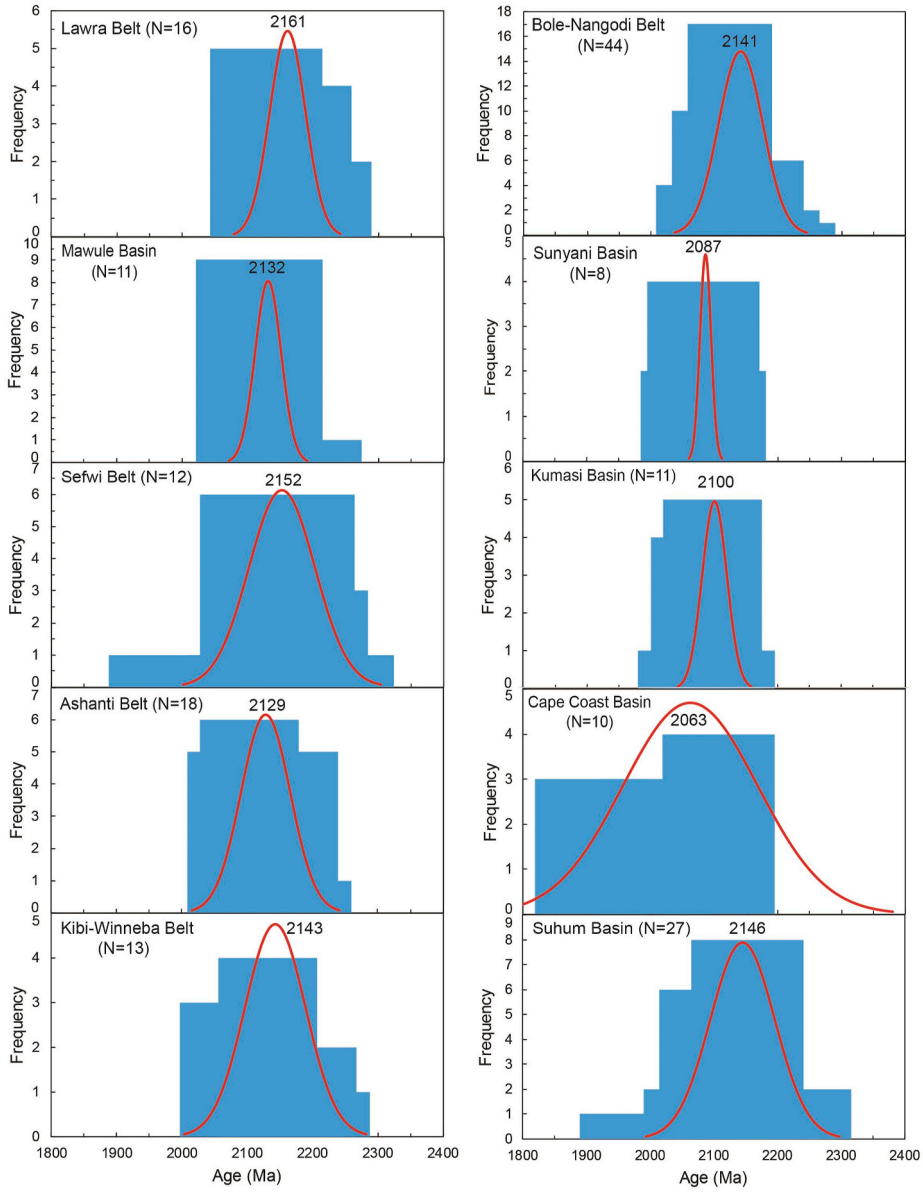

Fig. 13. Histograms of age data for belt- and basin-type Birimian granitoids, showing the frequencies of the ages. N represents the number of ages used. Data sources as in Fig. 11.

Table 4
Sm-Nd isotope data for Birimian granitoids of Ghana.

Sample	Rock type	Sm(ppm)	Nd(ppm)	Sm/Nd	$^{147}Sm/^{144}Nd$	$^{143}Nd/^{144}Nd$	εNd(t)	T_{DM1} (Ga)	T_{DM2} (Ga)	References
BOS10A	Muscovite granite	4.46	21.21	0.2103	0.1271	0.511818 ± 4	2.8	–	–	Losiak et al. (2013)
BOS10B	Muscovite granite	2.86	17.24	0.1659	0.1001	0.511461 ± 4	3.1	–	–	Losiak et al. (2013)
BOS11	Muscovite granite	2.71	17.35	0.1562	0.0943	0.511362 ± 4	2.8	–	–	Losiak et al. (2013)
BOS13	Mafic dike	2.90	11.54	0.2513	0.1521	0.512139 ± 12	2.3	–	–	Losiak et al. (2013)
BOS14A	Muscovite granite	2.54	16.94	0.1499	0.0905	0.51132 ± 4	3.0	–	–	Losiak et al. (2013)
BOS15	Muscovite granite	1.58	9.760	0.1619	0.0980	0.511452 ± 5	3.5	–	–	Losiak et al. (2013)
BOS16	Muscovite granite	2.92	16.53	0.1766	0.1067	0.511533 ± 4	2.7	–	–	Losiak et al. (2013)
BM01	Hornblende granite	21.68	122.2	0.1774	0.0932	0.51120	−0.16	2.45	2.32	Sakyi et al. (2020a)
BN01	Two-mica granite	5.00	37.20	0.1344	0.0733	0.51090	−0.65	2.43	2.31	Sakyi et al. (2020a)
RA01	Granite	7.25	61.77	0.1174	0.0711	0.51090	−0.05	2.39	2.27	Sakyi et al. (2020a)
TG01G	Granite	6.11	38.52	0.1586	0.0941	0.51120	−0.40	2.47	2.33	Sakyi et al. (2020a)
ZK04	Two-mica granite	4.17	25.34	0.1646	0.1030	0.51130	−0.86	2.53	2.39	Sakyi et al. (2020a)
RA08	Granitic gneiss	4.43	33.90	0.1307	0.0792	0.51100	−0.28	2.42	2.30	Sakyi et al. (2020a)
BS02	Adamellite	22.42	128.1	0.1750	0.0948	0.51130	1.37	2.36	2.22	Sakyi et al. (2020a)
NB01B	Granodiorite	3.22	17.87	0.1802	0.0951	0.51120	−0.67	2.49	2.35	Sakyi et al. (2020a)
BN03B	Granodiorite	10.00	64.29	0.1555	0.0808	0.51110	1.24	2.34	2.21	Sakyi et al. (2020a)
TG01E	Granodiorite	5.40	31.18	0.1732	0.0893	0.51120	0.90	2.38	2.24	Sakyi et al. (2020a)

εNd(t) calculated at 2077 Ma (Losiak et al., 2013) and 2100 Ma (Sakyi et al., 2020a).

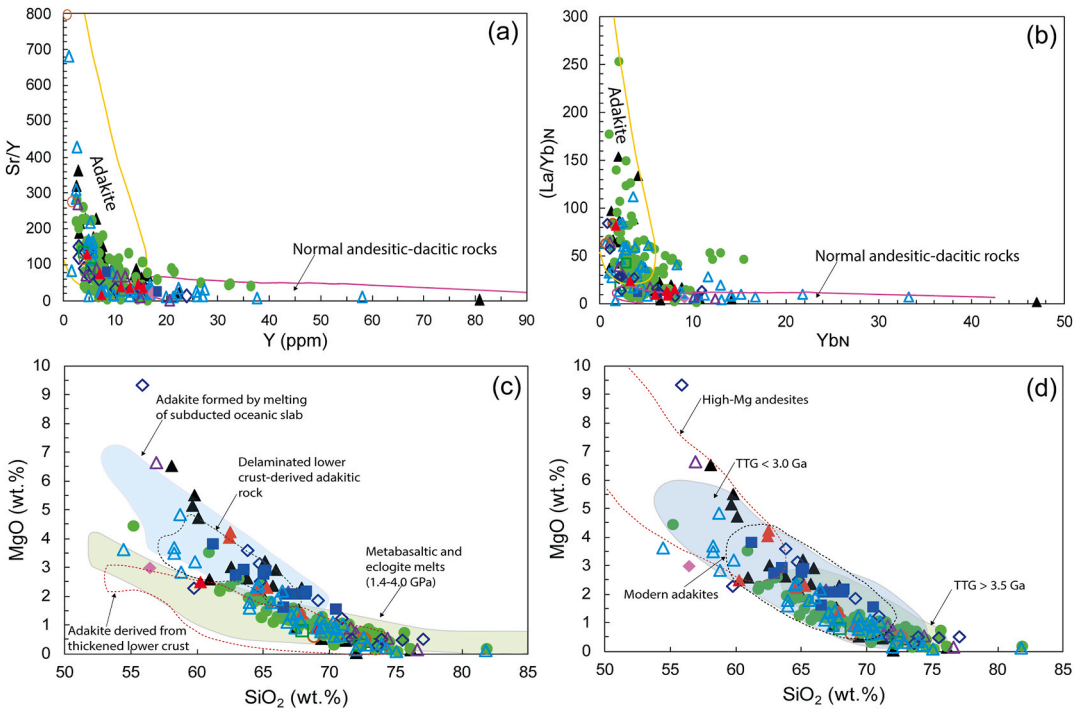

Fig. 14. Classification diagrams of (a) Sr/Y vs. Y and (b) $(La/Yb)_N$ vs. Yb_N (after Defant and Drummond, 1990) for the granitoid plutons and (c) MgO vs. SiO_2 diagram for the Birimian granitoids. Fields of TTG-like rocks derived from subducted oceanic crust, thickened lower crust, delaminated lower crust, and metabasalts/eclogites at pressures of 1.0–4.0 GPa are after Qin et al. (2015). (d) MgO vs. SiO_2 diagram showing the granitoids plotting in the TTG field (Hastie et al., 2010). Data symbols as in Fig. 6.

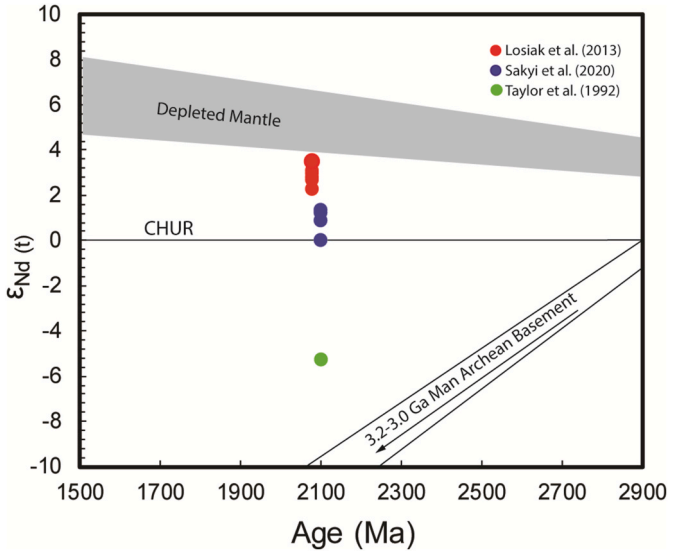

Fig. 15. εNd plots for Birimian granitoids in Ghana. Data from Taylor et at. (1992), Losiak et al. (2013), Sakyi et al. (2020a).

Fig. 17. This model takes into consideration the εHf signatures (Fig. 12) and peak ages (Fig. 13) recorded in the various belts and basins. The eastward subduction initiated partial melting of the basaltic crust (and lithospheric mantle) that interacted with the over-lying proposed thickened Archean crust (Fig. 17a). This magmatism led to the generation of magma with sub-chondritic εHf signatures, that formed a volcanic belt, with the maximum peak age of 2161 Ma (Fig. 18).

Subsequently, the subduction was followed by slab rollback (Fig. 17b) (e.g. Dilek and Flower, 2004). Slab rollback is considered to be the main mechanism controlling the rheology of the overriding plate (e.g. Schellart, 2008; Rey and Müller, 2010; Spakman and Hall, 2010; Butterworth et al., 2012). The slab rollback was associated with slab retreat and trench-ward magmatic migration (Kemp et al., 2009; Yumul Jr. et al., 2020) from a thickened retro-arc into a thinned extension zone where mantle derived magmas mixed with juvenile continental crust, generating melts with juvenile Hf isotope signatures (e.g., Kemp et al., 2009, Fig. 17b). Thus, the attenuation of the crust at the back-arc side with the diminishing influence of subduction led to an extensional phase, leading to the formation of several basins (Feybesse et al., 2006), potentially explaining the sudden return to supra-chondritic εHf signatures (Fig. 17b). In the thinned extensional zone, there was minimal interaction of the juvenile magma with the Archean crust, resulting in the general absence of sub-chondritic Hf signatures in most of the basin-type granitoids (Fig. 12b). The process produced alternating volcanic belts and sedimentary basins, with the belts recording higher peak ages relative to the basins (Fig. 17c).

These differences in the εHf values might reflect trench-ward magmatism characterized by little or no reworked Archean crust for the basins while retro-arc magmatism to the east involved reworked Archean crust for the belts. The subduction, slab rollback and extensional phase might have occurred in a relatively short time, producing the belts and basins with almost similar ages.

On the global scale, the Paleoproterozoic era (c.a. 2.5–1.6 Ga) witnessed the main episode of crustal growth that was recorded on present-day continents (Giustina et al., 2009). The Paleoproterozoic was marked by a sequence of geotectonic events, ultimately leading to the formation of orogenic belts and was characterized by large-scale collisional and post-collisional magmatic activities evidenced in most of the ancient cratons. It was also characterized by widespread mafic magmatism across previously stabilized Archean crustal domains (e.g., Heaman, 1997; Isley and Abbott, 1999). This global event was related to the assembly of the supercontinent Columbia in the Late Paleoproterozoic-Mesoproterozoic (e.g., Rogers and Santosh, 2002; Zhao et al., 2004; Meert, 2012), mainly at about c.a. 1.90–1.85 Ga (Rogers and Santosh, 2009). Zhao et al. (2002) proposed that the

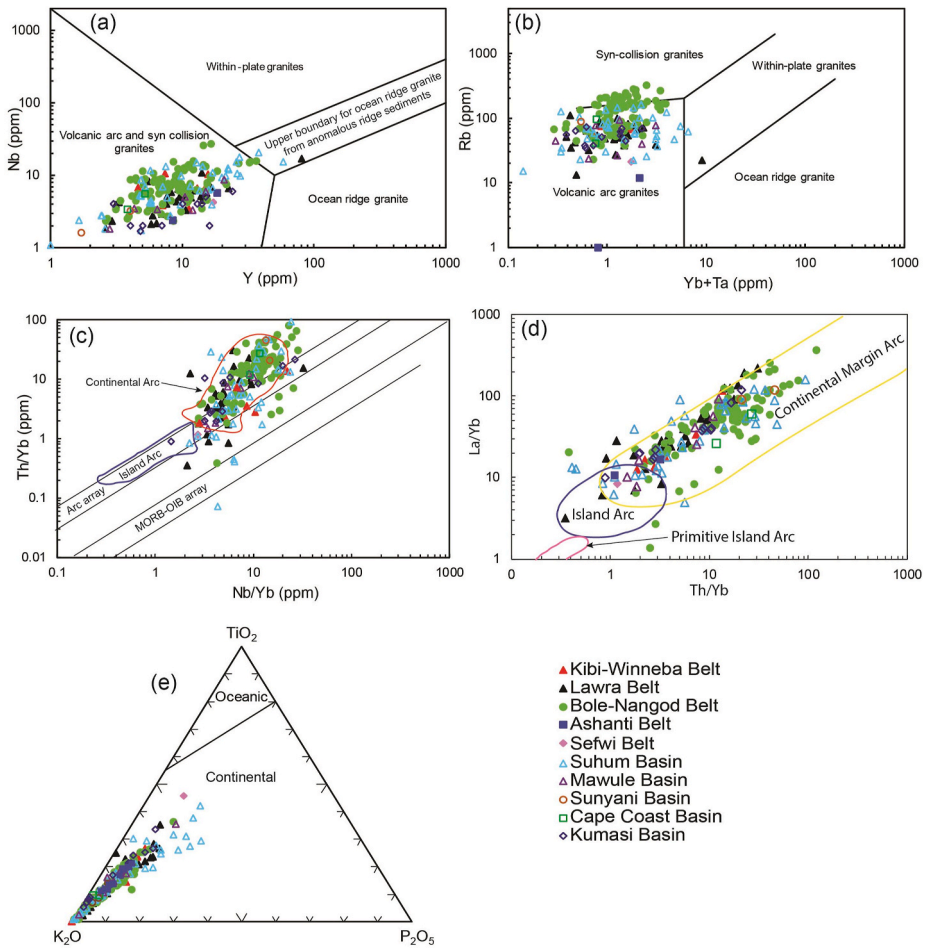

Fig. 16. (a) Nb vs. Y and (b) Rb vs. Yb + Ta tectonic discrimination diagrams (Pearce et al., 1984); (c) Th/Yb vs. Nb/Yb plot (modified after Pearce, 2008); (d) La/Yb vs. Th/Yb diagram (after Condie, 1989); (e) TiO_2-K_2O-P_2O_5 tectonic discrimination diagram (Pearce et al., 1975). VAG – volcanic-arc granite, Syn-COLG – syn-collision granite, WPG – within plate granite, ORG – ocean-ridge granite, Post-COLG – post-collision granite. Data sources as in Figs. 3 and 4.

assembly of the supercontinent Columbia (Nuna) was completed by global-scale collisional events during the Paleoproterozoic (c.a. 2.1–1.8 Ga). Rogers and Santosh (2002) advocated that between c.a. 1.9 and 1.5 Ga, South America formed part of West Africa whilst the eastern part of India was connected to the western part of North America, as part of Columbia. We therefore speculate that the subduction-accretion processes that prevailed in the Paleoproterozoic terrane of the WAC during the c.a. 2.1–2.0 Ga Eburnean orogeny makes the WAC a building block of the Columbia supercontinent.

4.4. Timing of emplacement

Several studies of the Birimian granitoids of Ghana have revealed different time spans for the emplacements of the granitoids, though with overlapping ages, in some cases (Table 1 and S2). Zircon U-Pb and Lu-Hf data from the Sefwi belt indicate contemporaneous emplacement of diorites and low-HREE TTGs between ca. 2159 and 2153 Ma whereas the high-K quartz monzonites were emplaced at ca. 2135 Ma (McFarlane et al., 2019b). The emplacement of high-P TTGs, granites and LILE-enriched diorites was probably due to lower crustal heating in response to the delamination of the lower crust and lithospheric mantle (Block et al., 2016b). Oberthür et al. (1998) published cyclic emplacement over ~ 110 million years (ca. 2190-2080 Ma) for granitic plutons in the Ashanti belt. Grenholm (2011) however, suggested the emplacement ages for the belt-type granitoids between ca. 2232-2169 Ma and for the basin-type granitoids between ca. 2134-2098 Ma. In the Lawra belt granitoid invasion spanned a period of ~81 Ma (ca. 2213-2130), though the data do not show any systematic emplacement of the rock types as their magmatic ages overlap (Sakyi et al., 2014). The Lawra and Bole-Nangodi Belts are therefore interpreted as an undifferentiated terrane that experienced an erratic emplacement of pulses of granitic magma of different compositions (Sakyi et al., 2014, 2020a), which is corroborated by de Kock et al. (2011) who showed that magmas can form simultaneously but in different tectonic environments. And unless its setting cannot be determined, it cannot be allocated to belt or basin intrusions to formulate the stratigraphic succession. The Kibi-Winneba belt in southeastern part of the Baoulé-Mossi domain also recorded emplacement over a period spanning ~70 Ma (Anum et al., 2015).

In the Suhum basin, the emplacement of protoliths of the amphibole-bearing gneisses, migmatitic gneisses and biotite gneiss which form the bulk of the studied rocks have an age bracket of ca. 2224-2137 Ma (~87 Ma) that corresponds to the timing of accretionary tectonism and magmatism. This led to the development of the first segments of the Paleoproterozoic Birimian continental crust (Amponsah et al., 2023). However, the U-Pb age ca. 2120 Ma for a leucosome segregate from a migmatitic gneiss could represent the very first approximate age of migmatisation in the Suhum basin. Nonetheless, with the intrusion of the leucogranite occurring around 2085 ± 110 Ma, the margin of error shows that the latter could have been synchronous with any of the amphibole-bearing gneiss, biotite gneiss and the migmatitic gneiss (Amponsah et al., 2023).

Furthermore, the data suggest simultaneous episodic emplacement of the granitoid bodies within a time-span of ~139 Ma in the Suhum basin, representing one of the most extensive periods of Eburnean-

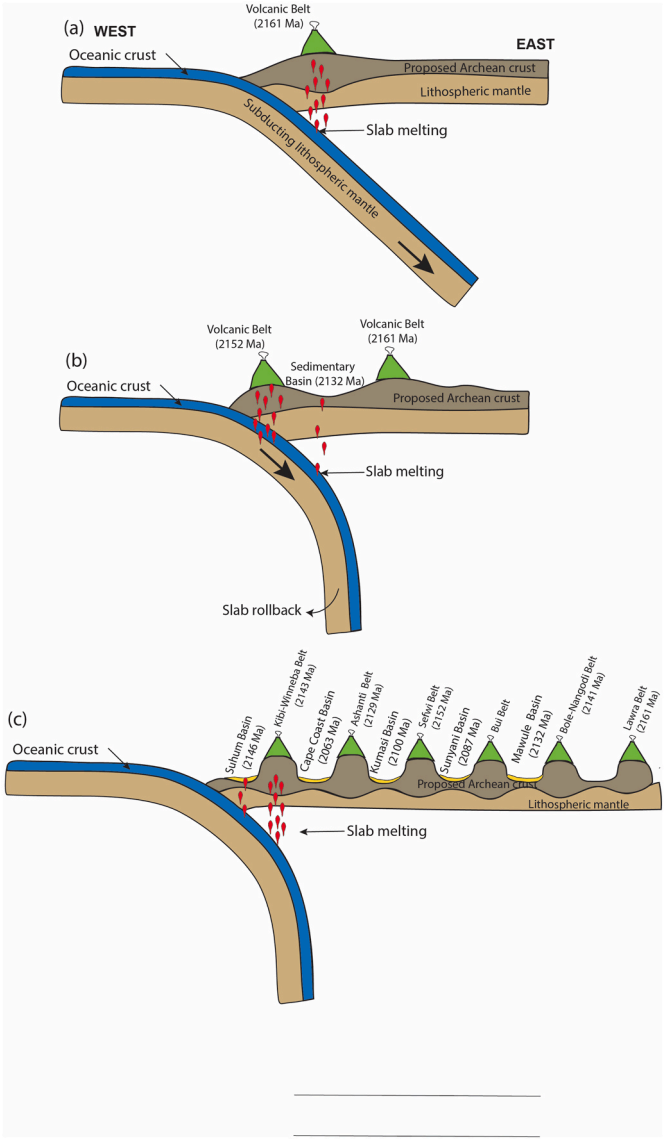

Fig. 17. Geodynamic tectonic model proposed for the evolution of the Birimian arc system in southeastern West African Craton. (a) The eastward subduction initiated partial melting of the basaltic crust (and lithospheric mantle) that interacted with the over-lying proposed thickened Archean crust. This generated magma with sub-chondritic εHf signatures, that formed a volcanic belt; (b) Subsequent slab rollback was accompanied by slab retreat and trench-ward magmatic migration from a thickened retro-arc into a thinned extension zone where mantle derived magmas mixed with juvenile continental crust, generating melts with juvenile Hf isotope signatures that erupted into the sedimentary several basins; (c) The process produced alternating volcanic belts and sedimentary basins, with the belts generally recording higher peak ages relative to adjacent basins. Peak ages as in Fig. 13.

related magmatism and plutonism recorded in Ghana and elsewhere in the southern WAC. The early-stage magmatism age of ca. 2224 Ma in the Suhum basin (Amponsah et al., 2023), further confirms that the oldest plutons with ages >2200 Ma are located mainly in the eastern margin of the Baoulé-Mossi domain (i.e., Burkina Faso and Ghana) (Tshibubudze et al., 2013, 2015; Sakyi et al., 2014; Block et al., 2016b; Petersson et al., 2016, 2018; Parra-Avila et al., 2017; Nunoo et al., 2022). Available data from northern Ghana indicate that the formation and emplacement of the granitic plutons occurred over an interval of ca. 100 Ma (ca. 2.2-2.1 Ga; Block et al., 2016b) and ca. 107 Ma (ca. 2181-2074 Ma; Sakyi et al., unpublished).

A holistic interpretation of these magmatic and emplacement time-

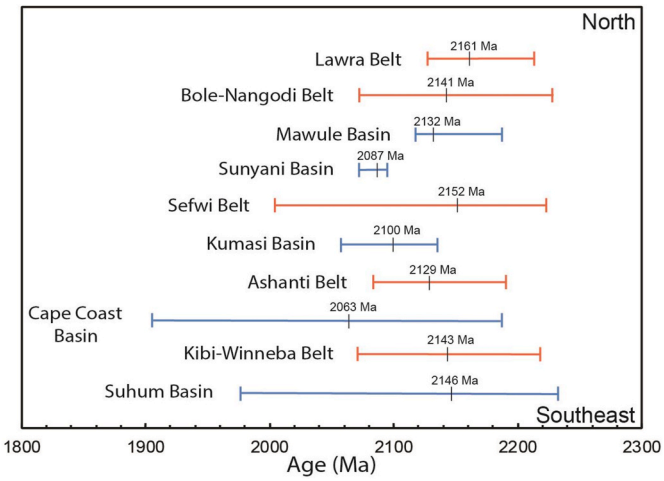

Fig. 18. Summarised graphical display of geochronological boundaries for the geological evolution of belt- and basin-type Birimian granitoids in Ghana. Peak ages in Fig. 13 are displayed. Data sources as in Fig. 11.

spans with respect to the various greenstone belts and sedimentary basins defines two conspicuous trends (Fig. 18). The available data show that: (i) the magmatic time-span is more prolong in southern Ghana (e.g., Sefwi belt-216 Ma; Ashanti belt-107 Ma; Kibi-Winneba belt-147 Ma; Cape Coast basin-280 Ma; Suhum basin-254 Ma), compared to the north (e.g., Lawra belt-85 Ma; Bole-Nangodi belt-154 Ma; Mawule basin-69 Ma), (ii) the longest magma emplacement intervals are recorded in the sedimentary basins (e.g., Cape Coast basin-280 Ma; Suhum basin-254 Ma), notably in the south. For the Cape Coast basin, even though a limited data of only 10 geochronological ages are currently available, it recorded the longest period of emplacement among all the belts and basins. This review work cannot immediately ascribe any reason to this observed trend. However, all the above-mentioned observations strongly indicate that magmatism in the southeastern part of the WAC might have taken place much earlier, with a prolonged period of emplacement.

5. Conclusion and recommendation

5.1. Conclusion

The crust of the Paleoproterozoic WAC in Ghana is dominantly made of tonalite- TTG suites, low-K to high-K calc-alkaline granites, LILE-enriched diorites, high-K quartz monzonites, two-mica granites and leucogranites. The granitoids are enriched in LILE and LREE relative to HREE and HFSE, and display negative Nb-Ta anomalies, pronounced negative Ti and P anomalies, and variable positive and negative Eu and Sr anomalies. There are generally positive anomalies of Rb, Ba, U, and Pb in all the samples, except the Ashanti and Sefwi belts, and the Cape Coast and Sunyani basins that do not have Pb data. Based on the available data, the plutons formed by partial melting of hydrous basaltic/mafic crust metasomatized mainly by slab-derived melts at differential depths of low temperatures and pressures. The εHf values of −14.5 to +7.6, εNd values of −5.3 to +3.5 and Nd model ages of 2.21–2.53 Ga indicate crystallization from juvenile liquids derived from a depleted mantle with significant involvement of older crustal material. The data strongly indicate that reworking of older crustal material was a common phenomenon in the genesis of the parental magma of the granitoids. The granitoids formed in a continental arc setting arising from subduction-accretion processes.

Older crystallization ages (≥2200 Ma) have been reported in the following greenstone belts and sedimentary basins; Lawra, Bole-Nangodi, Kibi-Winneba and Sefwi belts and the Suhum basin. Similarly, younger crystallization ages <2100 Ma have been reported for

granitoids from Ashanti and Kibi-Winneba belts, as well as the Cape Coast, Sunyani, Suhum and Kumasi basins. These age ranges strongly suggest that magma emplacement for both belt- and basin-type granitoids were contemporaneous. The magmatic time-span is more prolong in southern Ghana and the longest magma emplacement intervals are recorded in the sedimentary basins, which also recorded lower peak emplacement ages compared to the adjacent belts. Furthermore, the geochronological data show that inherited older zircon grains, interpreted to represent Archean zircon cores, are a widespread feature in the southeastern domain of the WAC.

The spatial variation in the εHf data and Hf model ages reveal predominantly sub-chondritic values towards the southeastern and northeastern parts of Ghana, and strongly suggest the existence of Neoarchean to Mesoarchean crustal material in eastern Ghana during the Birimian crust formation. We propose that the subduction-accretion processes that prevailed in the Paleoproterozoic terrane of the WAC during the c.a. 2.1–2.0 Ga Eburnean orogeny made the WAC a contributor to the buildup of the Columbia supercontinent in the Late Paleoproterozoic-Mesoproterozoic.

5.2. Recommendation

The Birimian terrane of Ghana comprises six greenstone belts and five sedimentary basins. However, the Bui belt lacks comparable data on the granitoids. This suggests that little or no study has been conducted on its plutonic bodies. It is therefore recommended that attention should be given to this belt in future studies to generate the required data to complement those of the remaining belts and basins to enable a holistic and comprehensive discussion on the Birimian plutonic suites in Ghana.

Considering their relatively large sizes of the Lawra, Sefwi and Kibi-Winneba belts, as well as the Cape Coast, Sunyani, Kumasi and Mawule basins, these terranes have limited geochemical, geochronological, and isotopic (Hf) data, and therefore may not be representative of the entire respective belts and basins, to warrant a meaningful comprehensive evaluation of past geologic activities. Future research should focus on these domains.

Lastly, with the exception of the Kumasi basin and Bole-Nangodi belt, the rest of the Birimian terrane in Ghana lack Nd isotope data on the granitoids. Future research works should focus on Nd isotope systematics. Future studies on the plutonic rocks should also employ K-isotope systematics since it is gaining widespread utilisation to investigate fractionation during granitic magmatism. Also, mineral chemistry is largely lacking in the database of Birimian granitoids in Ghana. Apart from limited EPMA data for a few terranes, trace elements data of common rock-forming minerals in granitoids is non-existing, and that is also a missing link in an attempt to understand the geochemical and geological evolution of the Birimian granitoids in southeastern part of the WAC. This therefore requires consideration in studies yet to be conducted. The implementation of the above-mentioned recommendations will help generate complete and robust database for studying the geodynamic evolution of the Birimian.

CRediT authorship contribution statement

Patrick Asamoah Sakyi: Writing – review & editing, Writing – original draft, Conceptualization. **Daniel Kwayisi:** Writing – review & editing, Software, Formal analysis, Data curation. **Samuel Nunoo:** Writing – review & editing, Software, Formal analysis. **Eric Ocran:** Software, Validation. **Ben-Xun Su:** Writing – review & editing, Writing – original draft, Conceptualization. **Sanjeewa P.K. Malaviarachchi:** Writing – review & editing, Writing – original draft, Formal analysis.

Declaration of competing interest

The authors declare that they have no known competing financial interests or personal relationships that could have appeared to influence the work reported in this paper.

Acknowledgments

This review benefitted from support from the Presidential International Fellowship Initiative (PIFI) awarded by the Chinese Academy of Sciences (CAS) to PAS. The authors are grateful to two anonymous reviewers for their comments on the previous versions of the manuscript that profoundly improved this version.

Appendix A. Supplementary data

Supplementary data to this article can be found online at https://doi.org/10.1016/j.jafrearsci.2024.105449.

Data availability

Data will be made available on request.

References

Abitty, E.K., Dampare, S.B., Nude, P.M., Daniel, K., Asiedu, D.K., 2016. Geochemistry and petrogenesis of the K-rich 'Bongo-type' granitoids in the Paleoproterozoic Bole-Nangodi greenstone belt of Ghana. J. African Earth Sci. 122, 47–62. https://10.1016/j.jafrearsci.2015.08.011.

Abouchami, W., Boher, M., Michard, A., Albarede, F., 1990. A major 2.1 Ga old event of mafic magmatism in West Africa: an early stage of crustal accretion. Geophys. Res. Lett. 95, 17605–17629. https://doi.org/10.1029/JB095iB11p17605.

Adadey, K., Théveniaut, H., Clarke, B., Urien, P., Delor, C., Roig, R.J., Feybesse, J.L., 2009. Geological Map Explanation, Map Sheet 0503B (1:100 000). CGS/BRGM/Geoman. Geological Survey Department, of Ghana.

Agra, N.A., Elburg, M.A., Vorster, C., 2023. Constraints on paleoproterozoic crustal growth from birimian Supergroup lavas of the Bui belt (Ghana) in the West African craton. Precambrian Res. 384, 106926. https://doi.org/10.1016/j.precamres.2022.106926.

Agyei-Duodu, J., Loh, G.K., Boamah, K.O., Baba, M., Anokwa, Y.M., Asare, C., Brakohiapa, E., Mensah, R.B., Okla, R., Toloczyki, M., Davis, D.W., Gluck, S., 2009. Geological Map of Ghana 1: 1 000 000. BSC, GGS, Accra (Ghana). Hannover (Germany).

Aidoo, F., Nude, P.M., Sun, F.-Y., Liang, T., Zhang, S.-B., 2021. Paleoproterozoic TTG-like metagranites from the Dahomeyide belt, Ghana: constraints on the evolution of the Birimian-Eburnean orogeny. Precambrian Res. 353, 106024. https://doi.org/10.1016/j.precamres.2020.106024.

Aidoo, F., Sun, F.-Y., Liang, T., Nude, P.M., 2020. New insight into the Dahomeyide belt of southeastern Ghana, West Africa: evidence of arc-continental collision and neoarchaean crustal reworking. Precambrian Res. 347, 105836. https://doi.org/10.1016/j.precamres.2020.105836.

Allibone, A.H., Mccuaig, C., Harris, D., Etheridge, M., Munroe, S., Byrne, D., Amanor, J., Gyapong, W., 2002a. Structural controls on gold mineralization at the Ashanti deposit, obuasi, Ghana. In: Goldfarb, R.J., Nielsen, R.L. (Eds.), Integrated Methods for Discovery: Global Exploration in the 21st Century, vol. 9. Spec. Publ. Soc. Econ. Geol., pp. 65–94. https://doi.org/10.5382/SP.09

Allibone, A., Teasdale, J., Cameron, G., Etheridge, M., Uttley, P., Soboh, A., Appiah-Kubi, J., Adanu, A., Arthur, R., Mamphey, J., Odoom, B., Zuta, J., Tsikata, A., Pataye, F., Famiyeh, S., Lamb, E., 2002b. Timing and structural controls on gold mineralization at the bogoso gold mine, Ghana, West Africa. Econ. Geol. 97 (5), 949–969.

Altherr, R., Holl, A., Hegner, E., Langer, C., Kreuzer, H., 2000. High potassium, calc-alkaline I-type plutonism in the European Variscides: northern Vosges (France) and northern Schwarzwald (Germany). Lithos 50, 51–73. https://doi.org/10.1016/S0024-4937(99)00052-3.

Ama Salah, I., Liégeois, J.-P., Pouclet, A., 1996. Evolution d'un arc insulaire océanique birimien précoce au Liptako nigérien (Sirba): géologie, géochronologie et géochemie. J. African Earth Sci. 22, 235–254. https://doi.org/10.1016/0899-5362(96)00016-4.

Amelin, Y., Lee, D.C., Halliday, Pidgeon, R.T., 1999. Nature of the Earth's earliest crust from hafnium isotopes in single detrital zircons. Nature 399, 252–255. https://doi.org/10.1038/20426.

Amelin, Y., Lee, D.-C., Halliday, A.N., 2000. Early-middle Archaean crustal evolution deduced from Lu-Hf and U-Pb isotopic studies of single grain zircons. Geochim. Cosmochim. Acta. 64, 4205–4225. https://doi.org/10.1016/S0016-7037(00)00493-2.

Amponsah, P.O., Kwayisi, D., Awunyo, E.K., Sapah, M.S., Sakyi, P.A., Su, B.-X., Lu, Y.-H., Nude, P.M., 2023. New evidence for crustal reworking and juvenile arc-magmatism during the Paleoproterozoic Eburnean events in the Suhum Basin, Southeast Ghana. Geol. J. 1–22. https://doi.org/10.1002/gj.4790.

Amponsah, P.A., Salvi, S., Beziat, D., Siebenaller, L., Jessell, M.W., 2015. Geology and geochemistry of the shear-hosted Julie gold deposit, NW Ghana. J. Afr. Earth Sci. 112, 505–523.

Anum, S., Sakyi, P.A., Su, B.X., Nude, P.M., Nyame, F., Asiedu, D., Kwayisi, D., 2015. Geochemistry and geochronology of granitoids in the Kibi-Asamankese area of the Kibi-Winneba volcanic belt, southern Ghana. J. African Earth Sci. 102, 166–179. https://doi.org/10.1016/j.jafrearsci.2014.11.007.

Arculus, R.J., Lapierre, H., Jaillard, É., 1999. Geochemical window into subduction and accretion processes; Raspas metamorphic complex, Ecuador. Geol. 27, 547–550.

Arndt, N.T., 2013. Formation and evolution of the continental crust. Geochem. Perspect. 2, 405–530. https://doi.org/10.7185/geochempersp.2.3.

Asiedu, D.K., Dampare, S.B., Sakyi, P.A., Banoeng-Yakubo, B., Osae, S., Nyarko, B.J.B., Manu, J., 2004. Geochemistry of Paleoproterozoic metasedimentary rocks from the Birim diamondiferous field, southern Ghana: implications for provenance and crustal evolution at the Archean-Proterozoic boundary. Geochem. J. 38, 215–228. https://doi.org/10.2343/geochemj.38.215.

Attoh, K., Ekwueme, B., 1997. The West african shield. Oxf. Monogr. Geol. Geophys. 35 (1), 517–528.

Azzouni-Sekkal, A., Bonin, B., Bowden, P., Bechiri-Benmerzoug, F., Meddi, Y., 2020. Zircon U–Pb and Lu–Hf isotopic systems in ediacaran to Fortunian "Taourirt" granitic ring complexes (Silet and in Tedeini terranes, Tuareg shield, Algeria). J. African Earth Sci. 168, 103865. https://doi.org/10.1016/j.jafrearsci.2020.103865.

Baratoux, L., Metelka, V., Naba, S., Jessell, M.W., Grégoire, M., Ganne, J., 2011. Juvenile Paleoproterozoic crust evolution during the Eburnean orogeny (~2.2–2.0 Ga), western Burkina Faso. Precambrian Res. 191, 18–45. https://doi.org/10.1016/j.precamres.2011.08.010.

Bassot, J.P., 1987. Le Complexe Volcano-Plutonique Calco-Alcali de la Rivière Daléma (Est Sénégal): Discussion de sa Signification Géodynamique dans le Cadre de L'Orogénie Eburnéenne (Protérozoïque Inférieur). J. African Earth Sci. 6, 505–519. https://doi.org/10.1016/0899-5362(87)90091-1.

Block, S., Baratoux, L., Zeh, A., Laurent, O., Bruguier, O., Jessell, M., Ailleres, L., Sagna, R., Parra-Avila, L.A., Bosch, D., 2016b. Paleoproterozoic juvenile crust formation and Stabilisation in the south-eastern West African craton (Ghana); new insights from U-Pb-Hf zircon data and geochemistry. Precambrian Res. 287, 1–30. https://doi.org/10.1016/j.precamres.2016.10.011.

Block, S., Ganne, J., Baratoux, L., Zeh, A., Parra-Avila, L.A., Jessel, M.W., Aillères, L., Siebenaller, L., 2015. African Craton. J. Metamorph. Geol. 33, 463–494.

Block, S., Jessell, M., Aillères, L., Baratoux, L., Bruguier, O., Zeh, A., Bosch, D., Caby, R., Mensah, E., 2016a. Lower crust exhumation during Paleoproterozoic (Eburnean) orogeny, NW Ghana, West African Craton: Interplay of coeval contractional deformation and extensional gravitational collapse. Precambrian Res. 274, 82–109. https://doi.org/10.1016/j.precamres.2015.10.014.

Boher, M., Abouchami, W., Michard, A., Albarède, F., Arndt, N., 1992. Crustal growth in West Africa at 2.1 Ga. J. Geophys. Res. 97, 345–369. https://doi.org/10.1029/91JB01640.

Bonin, B., Janoušek, V., Moyen, J.-F., 2020. Chemical variation, modal composition and classification of granitoids. Geol. Soc. Spec. Publ. 491, 9–51. https://doi.org/10.1144/SP491-2019-138.

Bouvier, A., Vervoort, J.D., Patchett, P.J., 2008. The Lu–Hf and Sm–Nd isotopic composition of CHUR: constraints from unequilibrated chondrites and implication for the bulk composition of terrestrial planets. Earth Planet Sci. Lett. 273, 48–57. https://doi.org/10.1016/j.epsl.2008.06.010.

Brenan, J.M., Shaw, H.F., Phinney, D.L., Ryerson, F.J., 1994. Rutile-aqueous fluid partitioning of Nb, Ta, Hf, Zr, U, and Th: implications for high field strength element depletions in island-arc basalts. Earth Planet Sci. Lett. 128, 327–339. https://doi.org/10.1016/0012-821X(94)90154-6.

Brenan, J.M., Shaw, H.F., Ryerson, F.J., Phinney, D.L., 1995. Mineral-aqueous fluid partitioning of trace elements at 900°C and 2.0 GPa: constraints on the trace element chemistry of mantle and deep crustal fluids. Geochim. Cosmochim. Acta 59, 3331–3350. https://doi.org/10.1016/0016-7037(95)00215-L.

Brown, M., 2013. Granite: from genesis to emplacement. Geol. Soc. Am. Bull. 125, 1079–1113. https://doi.org/10.1130/B30877.1.

Bruand, E., Storey, C., Fowler, M., Heilimo, E., 2019. Oxygen isotopes in titanite and apatite, and their potential for crustal evolution research. Geochim. Cosmochim. Acta 255, 144–162. https://doi.org/10.1016/j.gca.2019.04.002.

Butterworth, N.P., Quevedo, L., Morra, G., Muller, R.D., 2012. Influence of overriding plate geometry and rheology on subduction. Geochem. Geophys. Geosyst. 13, Q06W15. https://doi:10.1029/2011GC003968.

Caby, R., Delor, C., Agoh, O., 2000. Lithology, structure and metamorphism of the Birimian formations in the Odienné area (Ivory Coast): the major role played by plutonic diapirism and strike-slip faulting at the border of the Man Craton. J. Afr. Earth Sci. 30, 351–374.

Chalokwu, C.I., Ghazi, M.A., Eugene, E., Foord, E.E., 1997. Geochemical characteristics and K-Ar ages of rare-metal bearing pegmatites from the Birimian of southeastern Ghana. J. Afr. Earth Sci. 24, 1–9. https://doi.org/10.1016/S0899-5362(97)00022-5.

Champion, D.C., Sheraton, J.W., 1997. Geochemistry and Nd isotope systematics of Archaean granites in the Eastern Goldfields, Yilgarn Craton, Australia: implications for crustal growth models. Precambrian Res. 83, 109–132. https://doi.org/10.1016/S0301-9268(97)00007-7.

Chappell, B.W., White, A.J.R., 1974. Two contrasting granite types. Pacific Geol 8, 173–174.

Chappell, B.W., 1984. Source of S- and I-type granites in the Lachlan fold belt, southeastern Australia. Philos. Trans. Roy. Soc. Lond. A310, 693–707. https://doi.org/10.1017/S0263593300007720.

Chappell, B.W., 2004. Towards a unified model for granite genesis. Earth Sci. Trans. Roy. Soc. Edinb. 95, 1–10. https://doi.org/10.1017/s0263593300000870.

Chappell, B.W., White, A.J.R., 2001. Two contrasting granite types: 25 years later. Aust. J. Earth Sci. 48, 489–499. https://doi.org/10.1046/j.1440-0952.2001.00882.x.

Chappell, B.W., White, A.J.R., Wyborn, D., 1987. The importance of residual source material (restite) in granite petrogenesis. J. Petrol. 28, 1111–1138. https://doi.org/10.1093/petrology/28.6.1111.

Chappell, B.W., White, A.J., Hine, R., 1988. Granite provinces and basement terranes in the Lachlan fold belt, southeastern Australia. Aust. J. Earth Sci. 35, 505–521. https://doi.org/10.1080/08120099808729466.

Chen, S., Niu, Y., Sun, W., Zhang, Y., Li, J., Guo, P., Sun, P., 2015. On the origin of mafic magmatic enclaves (MMEs) in syn-collisional granitoids: evidence from the Baojishan pluton in the North Qilian Orogen, China. Mineral. Petrol. 109, 577–596. https://doi.org/10.1007/s00710-015-0383-5.

Clemens, W.D., Wall, V.J., 1984. Origin and evolution of peraluminous silicic ignimbrite suite: the Violet Town volcanics. Contrib. Mineral. Petrol. 88, 354–371. https://doi.org/10.1007/BF00376761.

Collins, W.J., 1996. Lachlan fold belt granitoids: products of three-component mixing. Trans. Roy. Soc. Edinb. Earth Sci. 87, 171–181. https://doi.org/10.1017/S0263593300006581.

Collins, W.J., Huang, H.Q., Bowden, P., Kemp, A.I.S., 2019. Repeated S–I–A-type granite trilogy in the Lachlan Orogen and geochemical contrasts with A-type granites in Nigeria: implications for petrogenesis and tectonic discrimination. Geol. Soc. Spec. Publ. 491, 53–76. https://doi.org/10.1144/SP491-2018-159.

Condie, K.C., 1989. Geochemical changes in basalts and andesites across the Archean–Proterozoic boundary: Identification and significance. Lithos 23, 1–18. https://doi.org/10.1016/0024-4937(89)90020-0.

Condie, K.C., O'Neill, C., Aster, R.C., 2009. Evidence and implications for a widespread magmatic shutdown for 250 My on Earth. Earth Planet Sci. Lett. 282 (1–4), 294–298. https://doi.org/10.1016/j.epsl.2009.03.033.

Condie, K.C., Beyer, E., Belousova, E., Griffin, W.L.O., Reilly, S.Y., 2005. U–Pb isotopic ages and Hf isotopic composition of single zircons: the search for juvenile Precambrian continental crust. Precambrian Res. 139, 42–100. https://doi.org/10.1016/j.precamres.2005.04.006.

Czarnota, K., Champion, D.C., Goscombe, B., Blewett, R.S., Cassidy, K.F., Henson, P.A., Groenewald, P.B., 2010. Geodynamics of the eastern yilgarn craton. Precambrian Res. 183 (2), 175–202. https://doi.org/10.1016/j.precamres.2010.08.004.

Dampare, S.B., Shibata, T., Asiedu, D.K., Osae, S., 2005. Major-element geochemistry of Proterozoic Prince's Town granitoid from the southern Ashanti volcanic belt, Ghana. Earth Sci. Rep. 12, 15–30.

Dampare, S.B., Shibata, T., Asiedu, D.K., Osae, S., Banoeng-Yakubo, B., 2008. Geochemistry of Paleoproterozoic metavolcanics rocks from the Southern Ashanti volcanic belt, Ghana: petrogenetic and tectonic setting implications. Precambrian Res. 162, 403–423. https://doi.org/10.1016/j.precamres.2007.10.001.

Davis, D.W., Hirdes, W., Schaltegger, U., Nunoo, E.A., 1994. U-Pb age constraints on deposition and provenance of Birimian and gold-bearing Tarkwaian sediments in Ghana, West Africa. Precambrian Res. 67, 89–107. https://doi.org/10.1016/0301-9268(94)90006-X.

de Kock, G.S., Armstrong, R.A., Siegfried, H.P., Thomas, E., 2011. Geochronology of the birim Supergroup of the West African craton in the wa-bolé region of West-central Ghana: implications for the stratigraphic framework. J. Afr. Earth Sci. 59, 1–40. https://doi.org/10.1016/j.jafrearsci.2010.08.001.

de Kock, G.S., Théveniaut, H., Botha, P.M.W., Gyapong, W., 2012. Timing the structural events in the Paleoproterozoic Bolé-Nangodi belt terrane and adjacent Maluwe basin, West African craton, in central-west Ghana. J. Afr. Earth Sci. 65, 1–24. https://doi.org/10.1016/j.jafrearsci.2011.11.007.

de Kock, M.O., Evans, D.A.D., Beukes, N.J., 2009. Validating the Existence of Vaalbara in the Neoarchean: Precambrian Res, vol. 174, pp. 145–154. https://doi.org/10.1016/j.precamres.2009.07.002.

Defant, M.J., Drummond, M.S., 1990. Derivation of some modern arc magmas by melting of young subducted lithosphere. Nature 347, 662–665. https://doi.org/10.1038/347662a0.

Deynoux, M., Affato, P., Trompette, R., Villeneuve, M., 2006. Pan-African tectonic evolution and glacial events registered in Neoproterozoic to Cambrian cratonic and foreland basins of West Africa. J. Afr. Earth Sci. 46, 397–426. https://doi.org/10.1016/j.jafrearsci.2006.08.005.

Dhuime, B., Hawkesworth, C.J., Cawood, P.A., Storey, C.D., 2012. A Change in the geodynamics of continental growth 3 billion years ago. Science 335, 1334–1336. https://doi.org/10.1126/science.1216066.

Dilek, Y., Flower, M.F.J., 2004. Arc-trench rollback and forearc accretion: 2. A model template for ophiolites in Albania, Cyprus and Oman. Geol. Soc. Spec. Publ. 218, 43–68. https://doi.org/10.1144/gsl.sp.2003.218.01.04.

Doumbia, S., Pouclet, A., Kouamelan, A., Peucat, J.J., Vidal, M., Delor, C., 1998. Petrogenesis of juvenile-type birimian (paleoproterozoic) granitoids in central côte-d'Ivoire, West Africa: geochemistry and geochronology. Precambrian Res. 87, 33–63. https://doi.org/10.1016/S0301-9268(97)00201-5.

Drummond, M.S., Defant, M.J., 1990. A model for trondhjemite-tonalite-dacite genesis and crustal growth via slab melting: Archean to Modern comparisons. J. Geophys. Res. 95, 21503–21521. https://doi.org/10.1029/JB095iB13p21503.

Egal, E., Thiéblemont, D., Lahondère, D., Guerrot, C., Costea, C.A., Iliescu, D., Delor, C., Goujou, J.-C., Lafon, J.M., Tegyey, M., Diaby, S., Kolié, P., 2002. Late eburnean granitization and tectonics along the western and northwestern margin of the archean kénéma–man domain (Guinea, West African craton). Precambrian Res. 117 (1–2), 57–84. https://doi.org/10.1016/S0301-9268(02)00060-8.

Eglinger, A., Thebaud, N., Zeh, A., Davis, J., Miller, J., Parra-Avila, L.A., Loucks, R., McCuaig, C., Belousova, E., 2017. New insights into crustal growth of the Paleoproterozoic margin of the Archaean Kemena-Man domain, West African craton (Guinea): implications of gold mineral system. Precambrian Res. 292, 258–289.

Eisenlohr, B.N., Hirdes, W., 1992. The structural development of the early Proterozoic Birimian and Tarkwaian rocks of southwest Ghana, West Africa. J. Afr. Earth Sci. 14, 313–325. https://doi.org/10.1016/0899-5362(92)90035-B.

Eleftheriadis, G., Koroneos, A., 2003. Geochemistry and petrogenesis of post-collision pangeon granitoids in Central Macedonia, northern Greece. Chem. Erde 63, 364–389. https://doi.org/10.1078/0009-2819-00024.

Ennih, N., Liégeois, J.P., 2008. The boundaries of the West African craton, with a special reference to the basement of the Moroccan metacratonic Anti-Atlas belt. In: Ennih, N., Liégeois, J.P. (Eds.), The Boundaries of the West African Craton, vol. 297. Geol. Soc. Spec. Publ., pp. 1–17. https://doi.org/10.1144/SP297.1

Feng, X., Wang, E., Ganne, J., Amponsah, P., Martin, R., 2018. Role of volcano-sedimentary basins in the formation of greenstone-granitoid belts in the West African craton: a numerical model. Minerals 8 (2), 73. https://doi.org/10.3390/min8020073.

Feybesse, J., Billa, M., Guerrot, C., Duguey, E., Lescuyer, J., Milési, J., Bouchot, V., 2006. The Paleoproterozoic Ghanaian province: geodynamic model and ore controls, including regional stress modelling. Precambrian Res. 149, 149–196. https://doi.org/10.1016/j.precamres.2006.06.003.

Feybesse, J.L., Milési, J.-P., 1994. The Archean/Paleoproterozoic contact zone in West Africa: a mountain belt of décollement thrusting and folding on a continental margin related to 2.1 Ga convergence of Archean cratons? Precambrian Res. 69, 199–227. https://doi.org/10.1016/0301-9268(94)90087-6.

Ganne, J., Gerbault, M., Block, S., 2014. Thermo-mechanical modeling of lower crustexhumation–constraints from the metamorphic record of the PalaeoproterozoicEburnean orogeny, West African Craton. Precambrian Res. 243, 88–109.

Gardiner, N.J., Kirkland, C.L., Kranendonk, M.J., 2016. The juvenile hafnium isotope signal as a record of Supercontinent cycles. Sci. Rep. 6, 38503.

Gasquet, D., Barbey, P., Adou, M., Paquette, J.L., 2003. Structure, Sr-Nd isotope geochemistry and zircon U-Pb geochronology of the granitoids of the Dabakala area (Cote d'Ivoire): evidence for a 2.3 Ga crustal growth event in the Palaeoproterozoic of West Africa? Precambrian Res. 127, 329–354.

Giustina, M.E.S.D., de Oliveira, C.G., Pimentel, M.M., de Melo, L.V., Fuck, R.A., Dantas, E.L., Buhn, B., 2009. U-Pb and Sm-Nd constraints on the nature of the Campinorte sequence and related Palaeoproterozoic juvenile orthogneisses, Tocantins Province, central Brazil. Geol. Soc. Spec. Publ. 323, 255–269.

Gong, S., He, C., Wang, X.C., Chen, N., Kusky, T., 2019. No plate tectonic shutdown in the early Paleoproterozoic: constraints from the ca. 2.4 Ga granitoids in the Quanji Massif, NW China. J. Asian Earth Sci. 172, 221–242.

Grenholm, M., 2011. Petrology of birimian granitoids in southern Ghana: petrography and petrogenesis. Bachelor Thesis, Department of Earth and Ecosystem Sciences, Division of Geology. Lund University.

Grenholm, M., Jessell, M., Nicolas Thebaud, T., 2019. Paleoproterozoic volcano-Sedimentary series in the ca. 2.27–1.96 Ga birimian orogen of the southeastern West African craton. Precambrian Res. 328, 161–192.

Griffin, W.L., Pearson, N.J., Belousova, E., Jackson, S.E., van Achterbergh, E., O'Reilly, S. Y., Shee, S.R., 2000. The Hf isotope composition of Cratonic mantle: LAM-MC-ICPMS analysis of zircon megacrysts in kimberlites. Geochem. Cosmochim. Acta 64 (1), 133–147. https://doi.org/10.1016/S0016-7037(99)00343-9.

Grove, T.L., Elkins-Tanton, L.T., Parman, S.W., Chatterjee, N., Müntener, O., Gaetani, G. A., 2003. Fractional crystallization and mantle-melting controls on calc-alkaline differentiation trends. Contrib. Mineral. Petrol. 145, 515–533.

Hastie, A.R., Kerr, A.C., McDonald, I., Mitchell, S.F., Pearce, J.A., Wolstencroft, M., Millar, I.L., 2010. Do Cenozoic analogues support a plate tectonic origin for Earth's earliest continental crust? Geology 38, 495–498.

Hawkesworth, C.J., Kemp, A.I.S., 2006. The differentiation and rates of generation of the continental crust. Chem. Geol. 226, 134–143.

Heaman, L.M., 1997. Global mafic magmatism at 2.45 Ga: remnants of an ancient large igneous province? Geology 25, 299–302.

Hein, K.A.A., 2010. Succession of structural events in the Goren greenstone belt (Burkina Faso): implications for West African tectonics. J. Afr. Earth Sci. 56, 83–94.

Hirdes, W., Davis, D.W., Eisenlohr, B.N., 1992. Reassessment of Proterozoic granitoid ages in Ghana on the basis of U/Pb-zircon and monazite dating. Precambrian Res. 56, 89–92.

Hirdes, W., Davis, D.W., 1998. First U-Pb zircon age of extrusive volcanism in the Birimian Supergroup of Ghana/West Africa. J. Afr. Earth Sci. 27, 291–294.

Hirdes, W., Davis, D.W., 2002. U–Pb geochronology of paleoproterozoic rocks in the southern part of the kedougou-kéniéba inlier, Senegal, West Africa: evidence for diachronous accretionary development of the eburnean province. Precambrian Res. 118 (1–2), 83–99.

Hirdes, W., Davis, D.W., Lüdtke, G., Konan, G., 1996. Two generations of Birimian (Paleoproterozoic) volcanic belts in northeastern Côte d'Ivoire (West Africa): consequences for the "Birimian controversy". Precambrian Res. 80, 173–191.

Hofmann, A.W., 1997. Mantle geochemistry: the message from oceanic volcanism. Nature 385, 219–229.

Irvine, T.N., Baragar, W.R.A., 1971. A guide to the chemical classification of the common volcanic rocks. Can. J. Earth Sci. 8, 523–548.

Isley, A.E., Abbott, D.H., 1999. Plume-related mafic volcanism and the deposition of banded iron formation. J. Geophys. Res. Solid Earth 104, 15461–15477.

Jagoutz, O., Klein, B., 2018. On the importance of crystallization-differentiation for the generation of SiO_2-rich melts and the compositional build-up of arc (and continental) crust. Am. J. Sci. 318, 29–63.

Janoušek, V., Moyen, J.-F., 2019. Whole-rock geochemical modelling of granite genesis: the current state of play. In: Janoušek, V., Bonin, B., Collins, W.J., Farina, F., Bowden, P. (Eds.), Post-archean Granitic Rocks: Petrogenetic Processes and Tectonic Environments, vol. 491. Geol. Soc. Spec. Publ. https://doi.org/10.1144/SP491-2018-160.

Jessell, M.W., Liégeois, J.P., 2015. 100 years of research on the West African craton. J. Afr. Earth Sci. 112, 377–381.

Kazapoe, R.W., Okunlola, O., Arhin, E., Olisa, O., Harris, C., Kwayisi, D., Torkorno, S., Amuah, E.E.Y., 2022. Geology and isotope systematics of gold deposits in the abansuoso area of the Sefwi belt, southwestern Ghana. Geol. Ecol. Landsc. https://doi.org/10.1080/24749508.2022.2142100.

Kazapoe, R.W., Okunlola, O., Arhin, E., Olisa, O., Kwayisi, D., Dzikunoo, E.A., Amuah, E. E.Y., 2023. Compositional characteristics of mineralised and unmineralised gneisses and schist around the Abansuoso area, southwestern Ghana. Appl. Earth Sci. 132 (1), 36–51.

Kearey, P., Klepeis, K.A., Vine, F.J., 2009. Global Tectonics, third ed. John Wiley & Sons, p. 496.

Kemp, A.I.S., Hawkesworth, C.J., Foster, G.L., Paterson, B.A., Woodhead, J.D., Hergt, J. M., Gray, C.M., Whitehouse, M.J., 2007. Magmatic and crustal differentiation history of granitic rocks from Hf-O isotopes in zircon. Science 315, 980–983.

Kemp, A.I.S., Hawkesworth, C.J., Collins, W.J., Gray, C.M., Belvin, P.L., EIMF, 2009. Isotopic evidence for rapid continental growth in an extensional accretionary orogen: the Tasmanides, eastern Australia. Earth Planet Sci. Lett. 284, 455–466. https://doi.org/10.1016/j.epsl.2009.05.011.

Keppler, H., 1996. Constraints from partitioning experiments on the composition of subduction-zone fluids. Nature 380, 237–240.

Kessel, R., Schmidt, M.W., Ulmer, P., Pettke, T., 2005. Trace element signature of subduction-zone fluids, melts and supercritical liquids at 120-180 km depth. Nature 437, 724–727.

Kogiso, T., Tatsumi, Y., Nakano, S., 1997. Trace element transport during dehydration processed in the subduction oceanic crust: 1. Experiments and implications for the origin of ocean island basalts. Earth Planet Sci. Lett. 148, 193–205.

Kouamelan, A.N., Djro, S.C., Allialy, M.E., Paquette, J.-L., Peucat, J.-J., 2015. The oldest rock of Ivory Coast. J. Afr. Earth Sci. 103, 65–70.

Kröner, A., Alexeiev, D.V., Rojas-Agramonte, Y., Hegner, E., Wong, J., Xia, X., Belousova, E., Mikolaichuk, A.V., Seltmann, R., Liu, D., Kiselev, V.V., 2013. Mesoproterozoic (Grenville-age) terranes in the Kyrgyz North Tianshan: zircon ages and Nd–Hf isotopic constraints on the origin and evolution of basement blocks in the southern Central Asian Orogen. Gondwana Res. 23 (1), 272–295.

Kwayisi, D., Amponsah, P. A., Awunyo, E. K., Sapah, M. S., Sakyi, P. A., Su, B.-X., Nude, P. M., Ayikwei, A. E., (Unpublished). Petrology and geochemistry of the Suhum Basin granitoid complex, Ghana: implications for crustal growth during the rhyacian orogeny of the West African craton. (In review, J. Afr. Earth Sci.: Manuscript ID: AES13103).

Laurent, O., Martin, H., Moyen, J.F., Doucelance, R., 2014. The diversity and evolution of late-Archaean granitoids: evidence for the onset of modern-style plate tectonics between 3.0 and 2.5 Ga. Lithos 205, 208–235.

Laurent, O., Zeh, A., 2015. A linear Hf isotope-age array despite different granitoid sources and complex Archean geodynamics: example from the Pietersburg block (South Africa). Earth Planet Sci. Lett. 430, 326–338.

Ledru, P., Johan, V., Milési, J.P., Tegyey, M., 1994. Markers of the last stages of the Paleoproterozoic collision: evidence for a 2.0 Ga continent evolving circum-South Atlantic provinces. Precambrian Res. 69, 169–191.

Leube, A., Hirdes, W., Mauer, R., Kesse, G.O., 1990. The Early Proterozoic Birimian Supergroup of Ghana and some aspects of its associated gold mineralization. Precambrian Res. 46, 139–165.

Liégeois, J.P., Claessens, W., Camara, D., Klerkx, J., 1991. Short-lived Eburnian orogeny in southern Mali. Geology, tectonics, U-Pb and Rb-Sr geochronology. Precambrian Res. 50, 111–136.

Liu, J., Liu, C., Deng, J., Luo, Z., He, G., Liu, Q., 2023. Igneous records of Mongolia–Okhotsk ocean subduction: evidence from granitoids in the Greater khingan mountains. Minerals 13, 493. https://doi.org/10.3390/min13040493.

Loh, G., Hirdes, W., Anani, C., Davis, D.W., Vetter, U., 1999. Explanatory notes for the geological map of Southwest Ghana 1: 100,000. Geologisches Jahrbuch B 93, 150.

Lompo, M., 2009. Geodynamic evolution of the 2.25-2.0 Ga Paleoproterozoic magmatic rocks in the Man-Leo Shield of the West African Craton. A model of subsidence of an oceanic plateau. Geol. Soc. Spec. Publ. 323, 231–254.

Losiak, A., Schulz, T., Buchwald, R., Koeberl, C., 2013. Petrology, major and trace element geochemistry, geochronology, and isotopic composition of granitic intrusions from the vicinity of the Bosumtwi impact crater, Ghana. Lithos 177, 297–313.

Lu, Y.-J., McCuaig, T.C., Li, Z.-X., Jourdan, F., Hart, C.J.R., Hou, Z.-Q., Tang, S.-H., 2015. Paleogene post-collisional lamprophyres in western Yunnan, western Yangtze craton: ante source and tectonic implications. Lithos 233, 139–161.

Luo, T., Liao, Q.A., Chen, J.P., Hu, C.B., Wang, F.M., Chen, S., Wu, W.W., Tian, J., Fan, G. M., 2017. A record of post-collisional transition: evidence from geochronology and geochemistry of Palaeozoic volcanic rocks in the eastern Junggar, Central Asia. Int. Geol. Rev. 59, 1256–1275.

Macpherson, C.G., Dreher, S., Thirlwall, M.F., 2006. Adakites without slab melting, Mindanao, the Philippines. Earth Planet Sci. Lett. 243, 581–593.

Maniar, P.D., Piccoli, P.M., 1989. Tectonic discrimination of granitoids. Geol. Soc. Am. Bull. 101 (5), 635–643.

Martin, H., 1987. Petrogenesis of Archaean trondhjemites, tonalites and granodiorites from eastern Finland: major and trace element geochemistry. J. Petrol. 28 (5), 921–953.

Matos, J.F., Kinney, S., Dorais, M.J., Christiansen, E.H., 2023. An εHf and $\delta^{18}O$ isotopic study of zircon of the mount osceola and conway granites, white mountain batholith, New Hampshire: deciphering the petrogenesis of A-type granites. Lithos 438–439, 106984.

McFarlane, H.B., 2018. The Geodynamic and Tectonic Evolution of the Palaeoproterozoic Sefwi Greenstone Belt, West African Craton (Ph.D. Thesis). Monash University.
McFarlane, H.B., Ailleres, L., Betts, P., Ganne, J., Baratoux, L., Jessell, M.W., Block, S., 2019a. Episodic collisional orogenesis and lower crust exhumation during the paleoproterozoic eburnean orogeny: evidence from the Sefwi greenstone belt, West African craton. Precambrian Res. 325, 88–110.
McFarlane, H.B., Thebaud, N., Parra-Avila, L.A., Armit, R., Spencer, C., Ganne, J., Ailleres, L., Baratoux, L., Betts, P.G., Jessell, M.W., 2019b. Onset of the supercontinent cycle: evidence for multiple oceanic arc accretion events in the paleoproterozoic Sefwi greenstone belt of the West African craton. Precambrian Res. 335, 105450.
Meert, J.G., 2012. What's in a name? The Columbia (Paleopangaea/Nuna) supercontinent. Gondwana Res. 21, 987–993.
Middlemost, E.A.K., 1994. Naming materials in magma/igneous rock system. Earth Sci. Rev. 37, 215–224.
Milési, J.P., Feybesse, J.L., Ledru, P., Dommanget, A., Ouedraogo, M.F., Marcoux, E., Prost, A., Vinchon, C., Sylvain, J.P., Johan, V., Tegyey, M., Calvez, J.Y., Lagny, P., 1989. Les minéralisations aurifères de l'Afrique de l'Ouest. Leur évolution lithostructurale au Protérozoïque inférieur. Notice et Carte à 1/2 000 000. Chron. Rech. Min. 497, 3–98.
Milési, J.P., Ledru, P., Feybbesse, J.L., Dommanget, A., Marcoux, E., 1992. Early Proterozoic ore deposits and tectonics of Birimian orogenic belt, West Africa. Precambrian Res. 58, 305–344.
Mo, X.X., Niu, Y.L., Dong, G.C., Zhao, Z.D., Hou, Z.Q., Zhou, S., Ke, S., 2008. Contribution of syncollisional felsic magmatism to continental crust growth: a case study of the Paleogene Linzizong volcanic succession in southern Tibet. Chem. Geol. 250 (1–4), 49–67.
Mortimer, J., 1992. The Kan River gneiss terrane of central Cote d'Ivoire: mylonitic remnants of an ancient magmatic arc? J. Afr. Earth Sci. 15, 353–367.
Moyen, J.-F., 2009. High Sr/Y and La/Yb ratios: the meaning of the "adakitic signature". Lithos 112, 556–574.
Moyen, J.-F., 2020. Granites and crustal heat budget. In: Janoušek, V., Bonin, B., Collins, W.J., Farina, F., Bowden, P. (Eds.), Post-archean Granitic Rocks: Petrogenetic Processes and Tectonic Environments, vol. 491. Geol. Soc. Spec. Publ., pp. 77–100
Moyen, J.F., Laurent, O., Chelle-Michou, C., Couzinié, S., Vanderhaeghe, O., Zeh, A., Villaros, A., Gardien, V., 2017. Collision vs. subduction-related magmatism: two contrasting ways of granite formation and implications for crustal growth. Lithos 277, 154–177.
Moyen, J.-F., Martin, H., 2012. Forty years of TTG research. Lithos 148, 312–336.
Niu, Y., Zhao, Z., Zhu, D.-C., Mo, X., 2013. Continental collision zones are primary sites for net continental crust growth–A testable hypothesis. Earth Sci. Rev. 127, 96–110.
Nunoo, S., Hofmann, A., Kramers, J., 2022. Geology, zircon U–Pb dating and εHf data for the Julie greenstone belt and associated rocks in NW Ghana: implications for Birimian-to-Tarkwaian correlation and crustal evolution. J. Afr. Earth Sci. 186, 104444.
Nyame, F.K., 2013. Origins of Birimian (ca 2.2 Ga) mafic magmatism and the Paleoproterozoic 'greenstone belt' metallogeny: a review. Isl. Arc 22, 538–548.
Oberthür, T., Vetter, U., Davis, D.W., Amanor, J.A., 1998. Age constraints on the gold mineralization and Paleoproterozoic crustal evolution in the Ashanti belt of southern Ghana. Precambrian Res. 89, 129–143.
O'connor, J.T., 1965. A classification for quartz-rich igneous rocks based on feldspar ratios. U. S. Geol. Surv. Prof. Pap. 525B, B79–B84.
Parra-Avila, L.A., Belousova, E., Fiorentini, M.L., Eglinger, A., Block, S., Miller, J., 2018. Zircon Hf and O-isotope constraints on the evolution of the paleoproterozoic baoulé-mossi domain of the southern West African craton. Precambrian Res. 306, 174–188.
Palme, H., O'Neill, H.St.C., 2014. Cosmochemical estimates of mantle composition. Treatise on Geochemistry 2, 1–39. Elsevier.
Parra-Avila, L.A., Baratoux, L., Eglinger, A., Fiorentini, M.L., Block, S., 2019. The eburnean magmatic evolution across the baoulé-mossi domain: geodynamic implications for the West African craton. Precambrian Res. 332, 105392.
Parra-Avila, L.A., Bourassa, Y., Miller, J., Perrouty, S., Fiorentini, M.L., McCuaig, T.C., 2015. Age constraints of the wassa and benso mesothermal gold deposits, Ashanti belt, Ghana, West Africa. J. Afr. Earth Sci. 112, 524–535.
Parra-Avila, L.A., Kemp, A.I.S., Fiorentini, M.L., Belousova, E., Baratoux, L., Block, S., Jessell, M., Bruguier, O., Begg, G.C., Miller, J., Davis, J., McCuaig, T.C., 2017. The geochronological evolution of the paleoproterozoic baoulé-mossi domain of the southern West African craton. Precambrian Res. 30, 1–27.
Pawlig, S., Gueye, M., Klischies, R., Schwarz, S., Wemmer, K., Siegesmund, S., 2006. Geochemical and Sr-Nd isotopic data on the birimian of the kedougou-kenieba inlier (eastern Senegal): implications on the palaeoproterozoic evolution of the West African craton. S. Afr. J. Geol. 109 (3), 411–427.
Pearce, J.A., 2008. Geochemical fingerprinting of oceanic basalts with applications to ophiolite classification and the search for Archean oceanic crust. Lithos 100 (1–4), 14–48. https://doi.org/10.1016/j.lithos.2007.06.016.
Pearce, J.A., Harris, N.B., Tindle, A.G., 1984. Trace element discrimination diagrams for the interpretation of granitic rocks. J. Petrol. 25, 957–983.
Pearce, J., 1996. Sources and setting of granitic rocks. Episode 19 (4), 120–125.
Pearce, T.H., Gorman, B.E., Birkette, T.C., 1975. The TiO_2-K_2O-P_2O_5 diagram: a method of discriminating between oceanic and non-oceanic basalts. Earth Planet Sci. Lett. 24 (3), 419–426.
Peccerillo, A., Taylor, S.R., 1976. Geochemistry of Eocene calc-alkaline volcanic rocks from the Kastamonu area, northern Turkey. Contrib. Mineral. Petrol. 58 (1), 63–81.
Perrouty, S., Aillères, L., Jessell, M., Baratoux, L., Bourassa, Y., Crawford, B., 2012. Revised Eburnean geodynamic evolution of the gold-rich southern Ashanti Belt, Ghana, with new field and geophysical evidence of pre-Tarkwaian deformations. Precambrian Res. 204–205, 12–39.
Petersson, A., Scherstén, A., Gerdes, A., 2018. Extensive reworking of Archaean crust within the Birimian terrane in Ghana as revealed by combined zircon U-Pb and Lu-Hf isotopes. Geosci. Front. 9 (1), 173–189.
Petersson, A., Scherstén, A., Kemp, A.I.S., Kristinsdóttir, B., Kalvig, P., Anum, S., 2016. Zircon U-Pb-Hf evidence for subduction related crustal growth and reworking of Archaean crust within the Palaeoproterozoic Birimian terrane, West African Craton, SE Ghana. Precambrian Res. 275, 286–309.
Peucat, J.-J., Capdevila, R., Drareni, A., Mahdjoub, Y., Kahoui, M., 2005. The Eglab massif in the West African Craton (Algeria), an original segment of the Eburnean orogenic belt: petrology, geochemistry and geochronology. Precambrian Res. 136, 309–352.
Pigois, J.P., Groves, D.I., Fletcher, I.R., McNaughton, N.J., Snee, L.W., 2003. Age constraints on Tarkwaian paleoplacer and lode-gold formation in the Tarkwa-Damang district, SW Ghana. Miner. Depos. 38, 695–714.
Pohl, D., 1998. A decade of change-mineral exploration in West Africa. The J. South Afr. Inst. Min. Metall. 98, 311–316.
Pohl, D., Carlson, C., 1993. A plate tectonic re-interpretation of the 2.2-2.0 Ga Birimian province, Tarkwaian System and metallogenesis in West Africa. In: Peters, J.W., Kesse, G.O., Acquah, P.C. (Eds.), Regional Trends in African Geology, Geol. Soc. Afr. Accra, pp. 378–381.
Pons, J., Barbey, P., Dupuis, D., Leger, J.M., 1995. Mechanisms of pluton emplacement and structural evolution of a 2.1 Ga juvenile continental crust: the Birimian of southwestern Niger. Precambrian Res. 70, 281–301.
Pouclet, A., Doumbia, S., Vidal, M., 2006. Geodynamic setting of the birimian volcanism in central ivory Coast (western Africa) and its place in the palaeoproterozoic evolution of the man shield. Bull. Soc. Geol. Fr. 177 (2), 105–121.
Pouclet, A., Vidal, M., Delor, C., Siméon, Y., Alric, G., 1996. Le volcanisme birimien du nord-est de la Côte-d'Ivoire, mise en évidence de deux phases volcanotectoniques distinctes dans l'évolution géodynamique du Paléoprotérozoïque. Bull. Soc. Geol. Fr. 167 (4), 529–541.
Qin, Z., Wu, Y., Siebel, W., Gao, S., Wang, H., Abdallsamed, M.I.M., Zhang, W., Yang, S., 2015. Genesis of adakitic granitoids by partial melting of thickened lower crust and its implications for early crustal growth: a case study from the Huichizi pluton, Qinling orogen, central China. Lithos 238, 1–12. https://doi.org/10.1016/j.lithos.2015.09.017.
Rapp, R., Shimizu, N., Norman, M.C., Applegate, G.S., 2000. Reaction between slab-derived melts and peridotite in the mantle wedge: experimental constraints at 3.8 GPa. Chem. Geol. 160, 335–356.
Rey, P.F., Müller, R.D., 2010. Fragmentation of active continental plate margins owing to the buoyancy of the mantle wedge. Nat. Geosci. 3, 257–261.
Rino, S., Komiya, T., Windley, B., Katayama, I., Motoki, A., Hirata, T., 2004. Major episodic increases of continental crustal growth determined from zircon ages of river sands: implications for mantle overturns in the Early Precambrian. Phys. Earth Planet. Inter. 146, 369–394.
Roberts, N.M.W., 2012. Increased loss of continental crust during supercontinent amalgamation. Gondwana Res. 21, 994–1000.
Robertson, M., Peters, L., 2016. West african goldfields. Episodes 39, 155–176.
Rogers, J.J.W., Santosh, M., 2002. Configuration of Columbia, a mesoproterozoic supercontinent. Gondwana Res. 5, 5–22.
Rogers, J.J.W., Santosh, M., 2009. Tectonics and surface effects of the supercontinent Columbia. Gondwana Res. 15, 373–380.
Roverato, M., Giordano, D., Giovanardi, T., Juliani, C., Polo, L., 2019. The 2.0–1.88 Ga Paleoproterozoic evolution of the southern Amazonian Craton (Brazil): an interpretation inferred by lithofaciological, geochemical and geochronological data. Gondwana Res. 70, 1–24.
Rudnick, R.L., Gao, S., 2003. Composition of the continental crust. In: Turekian, H.D.H.K. (Ed.), Treatise on Geochemistry. Pergamon, Oxford, pp. 1–64.
Rudnick, R.L., Gao, S., 2014. Composition of the continental crust. In: Holland, H.D., Turekian, K.K. (Eds.), Treatise on Geochemistry, second ed. Elsevier-Pergamon, Oxford, pp. 1–51.
Sakyi, P.A., Anum, S., Su, B.-X., Nude, P.M., Su, B.-C., Asiedu, D.K., Nyame, F., Kwayisi, D., 2018. Geochemical and Sr-Nd isotopic records of Paleoproterozoic metavolcanics and mafic intrusive rocks from the West African Craton: evidence for petrogenesis and tectonic setting. Geol. J. 52, 725–741.
Sakyi, P.A., Manu, M., Su, B.-X., Kwayisi, D., Nude, P.M., Dampare, S.B., 2019. Geochemical and Sm–Nd isotopic evidence for the composition of the palaeoproterozoic crust of the West African craton in Ghana. Geol. J. 54, 3940–3957.
Sakyi, P.A., Su, B.X., Anum, S., Kwayisi, D., Dampare, S.B., Anani, C.Y., Nude, P.M., 2014. New zircon U-Pb ages for erratic emplacement of 2213-2130 Ma paleoproterozoic calc-alkaline I-type granitoid rocks in the Lawra volcanic belt of northwestern Ghana, West Africa. Precambrian Res. 254, 149–168.
Sakyi, P.A., Su, B.-X., Manu, J., Kwayisi, D., Anani, C.Y., Alemayehu, M., Malaviarachchi, S.P.K.D., Nude, P.M., Su, B.-C., 2020b. Origin and tectonic significance of the metavolcanic rocks and mafic enclaves from the palaeoproterozoic birimian terrane, SE West African craton, Ghana. Geol. Mag. 157, 1349–1366.
Sakyi, P.A., Addae, R.A., Su, B.X., Dampare, S.B., Abitty, E., Su, B.C., Liu, B., Asiedu, D. K., 2020a. Petrology and geochemistry of TTG and K-rich paleoproterozoic birimian granitoids of the West African craton (Ghana): petrogenesis and tectonic implications. Precambrian Res. 336, 105492.
Sawyer, E.W., Cesare, B., Brown, M., 2011. When the continental crust melts. Elements 7, 229–234.
Schellart, W.P., 2008. Subduction zone trench migration: slab driven or overriding plate-driven? Phys. Earth Planet. Inter. 170, 73–88.

Senyah, G.A., Dampare, S.B., Asiedu, D.K., 2016. Geochemistry and tectonic setting of the paleoproterozoic metavolcanic rocks from the chirano gold district, Sefwi belt, Ghana. J. Afr. Earth Sci. 122, 32–46.

Sial, A.N., Bettencourt, J.S., De Campos, C.P., Ferreira, V.P., 2011. Granite-related ore deposits. Geol. Soc. Spec. Publ. 350. https://doi.org/10.1144/SP350.

Soesoo, A., 2000. Fractional crystallization of mantle-derived melts as a mechanism for some I-type granite petrogenesis: an example from the Lachlan Fold Belt, Australia. J. Geol. Soc. 157, 135–149. https://doi.org/10.1144/jgs.157.1.135.

Spakman, W., Hall, R., 2010. Surface deformation and slab-mantle interaction during Banda arc subduction rollback. Nat. Geosci. 3, 562–566. https://doi.org/10.1038/NGE0917.

Spencer, C.J., Kirkland, C.L., Prave, A.R., Strachan, R.A., Pease, V., 2019. Geoscience Frontiers Crustal reworking and orogenic styles inferred from zircon Hf isotopes: Proterozoic examples from the North Atlantic region. Geosci. Front. 10 (2), 417–424.

Sylvester, P.J., Attoh, K., 1992. Lithostratigraphy and composition of 2.1 Ga greenstone belts of the West African craton and their bearing on crustal evolution and Archean–Proterozoic boundary. J. Geol. 100, 377–393.

Tang, Y.-W., Chen, L., Zhao, Z.-F., Zheng, Y.-F., 2021. Origin of syn-collisional granitoids in the Gangdese orogen: reworking of the juvenile arc crust and the ancient continental crust. Geol. Soc. Am. Bull. 134 (3–4), 577–598.

Tatsumi, Y., Hamilton, D.L., Nesbitt, R.W., 1986. Chemical characteristics of fluid phase released from a subducted lithosphere and origin of arc magmas: evidence from high-pressure experiments and natural rocks. J. Volcanol. Geotherm. Res. 29, 293–309.

Taylor, N.P., Moorbath, S., Leube, A., Hirdes, W., 1992. Early Proterozoic crustal evolution in the Birimian of Ghana: constraints from geochronology and isotope geochemistry. Precambrian Res. 56, 97–111.

Taylor, S.R., McLennan, S.M., 2009. Planetary Crusts: Their Composition and Evolution. Cambridge University Press, Cambridge, p. 378.

Thiéblemont, D., Goujou, J.C., Egal, E., Cocherie, A., Delor, C., Lafon, J.M., Fanning, C. M., 2004. Archean evolution of the Leo rise and its Eburnean reworking. J. Afr. Earth Sci. 39, 97–104.

Tshibubudze, A., Hein, K.A.A., McCuaig, T.C., 2015. The relative and absolute chronology of strato-tectonic events in the Gorom-Gorom granitoid terrane and Oudalan-Gorouol belt, northeast Burkina Faso. J. Afr. Earth Sci. 112, 382–418.

Tshibubudze, A., Hein, K.A.A., Peters, L.F.H., Woolfe, A.J., McCuaig, T.C., 2013. Oldest U-Pb crystallisation age for the West African craton from the oudalan-gorouol belt of Burkina Faso. S. Afr. J. Geol. 116 (1), 169–181.

Ustaömer, T., Ustaömer, P.A., Robertson, A.H.F., Gerdes, A., 2016. Implications of U–Pb and Lu–Hf isotopic analysis of detrital zircons for the depositional age, provenance and tectonic setting of the Permian-Triassic Palaeotethyan Karakaya Complex, NW Turkey. Int. J. Earth Sci. 105 (1), 7–38.

Vidal, M., Gumiaux, C., Cagnard, F., Pouclet, A., Ouattara, G., Pichon, M., 2009. Evolution of a paleoproterozoic "weak type" orogeny in the West African craton (ivory Coast). Tectonophysics 477 (3–4), 145–159.

Villeneuve, M., Cornée, J.J., 1994. Structure, evolution and palaeogeography of the West African craton and bordering belts during the Neoproterozoic. Precambrian Res. 69 (1–4), 307–326.

Whalen, J.B., Currie, K.L., Chappell, B.W., 1987. A-type granites: geochemical characteristics, discrimination and petrogenesis. Contrib. Mineral. Petrol. 95 (4), 407–419.

White, A.J.R., Chappell, B.W., 1983. Granitoid types and their distribution in the Lachlan Fold Belt, southeastern, Australia. In: Roddick, J.A. (Ed.), Circum-Pacific Plutonic Terranes. Mem. Geol. Soc. Am, vol. 159, pp. 21–34.

Wright, J.B., Hastings, D.A., Jones, W.B., Williams, H.R., 1985. Geology and Mineral Resources of West Africa. George Allen and Unwin, Boston, p. 187.

Wu, F.Y., Liu, X.C., Ji, W.Q., Wang, J.M., Yang, L., 2017. Highly fractionated granites: recognition and research. Sci. China Earth Sci. 60, 1201–1219.

Xiao, Y., Chen, S., Niu, Y., Wang, X., Xue, Q., Wang, G., Gao, Y., Gong, H., Kong, J., Shao, F., Sun, P., Duan, M., Hong, D., Wang, D., 2020. Mineral compositions of syncollisional granitoids and their implications for the formation of juvenile continental crust and adakitic magmatism. J. Petrol. 61 (3), egaa038. https://doi:10.1093/petrology/egaa038.

Yumul, Jr.G.P., Dimalanta, C.B., Salapare, R.C., Queaño, K.L., Faustino-Eslava, D.V., Marquez, E.J., Ramos, N.T., Payot, B.D., Guotana, J.M.R., Gabo-Ratio, J.A.S., Armada, L.T., Padrones, J.T., Ishida, K., Suzuki, S., 2020. Slab rollback and microcontinent subduction in the evolution of the Zambales Ophiolite Complex (Philippines): a review. Geosci. Front. 11, 23–36.

Zhang, G.L., Zhang, J., Dalton, H., Phillips, D., 2022. Geochemical and chronological constraints on the origin and mantle source of early cretaceous arc volcanism on the gagua ridge in western pacific. Geochem. Geophys. Geosyst. 23, e2022GC010424. https://doi.org/10.1029/2022GC010424.

Zhao, G., Cawood, P.A., Wilde, S.A., Sun, M., 2002. Review of global 2.1–1.8 Ga collisional orogens and accreted cratons: a pre-Rodinia supercontinent? Earth Sci. Rev. 59, 125–162.

Zhao, G., Sun, M., Wilde, S.A., Li, S., 2004. A Paleo-Mesoproterozoic supercontinent: assembly, growth, and breakup. Earth Sci. Rev. 67, 91–123.

Zheng, Y.-F., 2019. Subduction zone geochemistry. Geosci. Front. 10, 1223–1254.

Zheng, Y.-F., Gao, P., 2021. The production of granitic magmas through crustal anatexis at convergent plate boundaries. Lithos 402–403, 106232. https://doi.org/10.1016/j.lithos.2021.106232.

Zhong, S., Li, S., Liu, Y., Cawood, P.A., Seltmann, R., 2023. I-type and S-type granites in the Earth's earliest continental crust. Commun. Earth Environ. 4, 61. https://doi.org/10.1038/s43247-023-00731-7.